EP 2009-02

Assessment of the mineral potential for porphyry Cu-Au ± Mo deposits in the Baie-James region

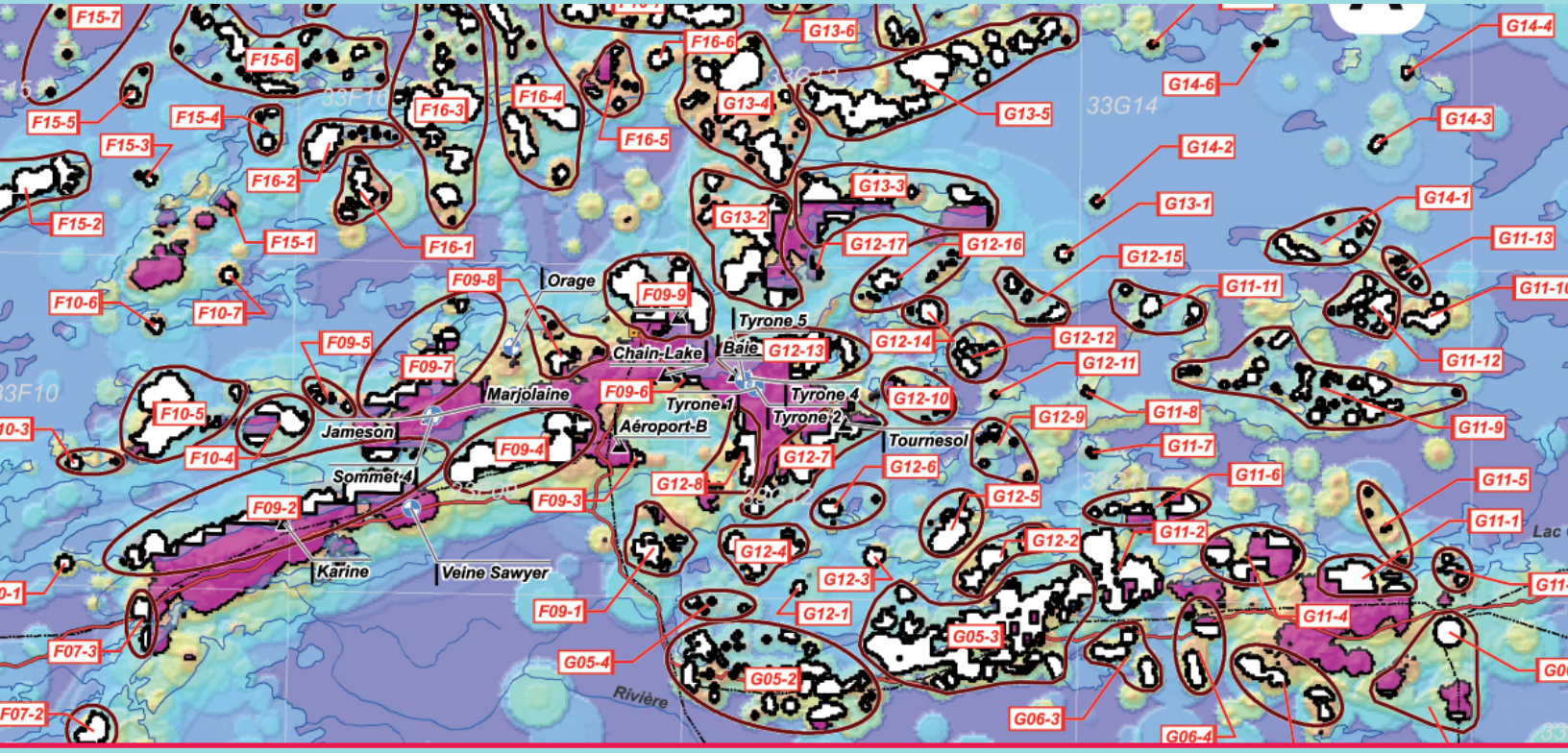

Daniel Lamothe

2009

Québec

Assessment of the mineral potential for porphyry Cu-Au ± Mo deposits in the Baie-James region

Daniel Lamothe

EP 2009-02

Keywords: favourability, porphyry deposits, Cu-Au ± Mo, Baie-James, targets

DOCUMENT PUBLISHED BY GÉOLOGIE QUÉBEC

Direction générale de Géologie Québec
Robert Marquis

Direction de l'information géologique
Pierre Verpaelst

Editing
Denis L. Lefebvre, P. Eng.

Graphic Design
Charlotte Grenier

Document accepted for publication January 27, 2009

Dépôt légal - Bibliothèque et Archives nationales du Québec, 2009
ISBN : 978-2-550-55630-5

Abstract

The purpose of this study is to determine the location of high-favourability zones for porphyry Cu-Au ± Mo deposits in the Baie-James region. High-favourability zones are defined based on 32 parameters grouped into 5 broad categories, namely: 1) presence of a heat source; 2) lithological control; 3) structural control; 4) hydrothermal activity; and 5) evidence in the secondary environment.

The geological relevance of each parameter is weighed using the Weight of Evidence spatial analysis method. This "geoprocessing" measures the probability of spatial association for each parameter with a weighing set of 61 porphyry Cu-Au ± Mo deposits derived from the total number of 72 known porphyry deposits within the study area. Calculated weight factors are then converted into fuzzy values and parameters are combined using a fuzzy logic approach.

A minimum favourability threshold was established using a statistical approach in order to delineate high-favourability zones. These zones encompass 80.5% of the 72 known porphyry deposits in the Baie-James region. By eliminating from these zones staked lands as of November 1, 2008, the author identified 198 new targets open to exploration.

TABLE OF CONTENTS

ATTACHMENTS

93 potential assessment maps for porphyry Cu-Au ± Mo deposits in the Baie-James region:

1 map at 1/500,000 scale……Map EP 2009-01 C001

12 maps at 1/250,000 scale……(32I, 32J, 32K, 32N, 32O, 32P, 33A, 33B, 33C, 33F, 33G, 33H)

80 maps at 1/50,000 scale……..(32I04, 32I05, 32J01, 32J09, 32J10, 32J11, 32J12, 32J15, 32J16, 32K01, 32K02, 32K09, 32K12, 32K15, 32K16, 32O01, 32O02, 32O12, 32O13, 32O14, 32P15, 32P16, 33A01, 33A03, 33A07, 33A08, 33A16, 33B01, 33B03, 33B04, 33B05, 33B06, 33B07, 33B08, 33B09, 33B10, 33B12, 33B13, 33B15, 33B16, 33C01, 33C02, 33C03, 33C04, 33C05, 33C06, 33C07, 33C08, 33C09, 33C10, 33C11, 33C12, 33C15, 33C16, 33F02, 33F03, 33F04, 33F05, 33F06, 33F07, 33F09, 33F10, 33F11, 33F12, 33F13, 33F15, 33F16, 33G03, 33G04, 33G05, 33G06, 33G08, 33G09, 33G10, 33G11, 33G12, 33G13, 33G14, 33G16, 33H09)

INTRODUCTION

The advent in the early 1990s of GIS (Geographic Information System) platforms led to the development of various approaches to process and combine multiple geological parameters in order to define zones favourable for the exploration of economic commodities (Chung and Agterberg, 1980; Bonham-Carter *et al.*, 1988; Harris, 1989; Agterberg *et al.*, 1990; Chung and Moon, 1991; Bonham-Carter, 1994; Rencz *et al.*, 1994; Harris *et al.*, 1995; Wright and Bonham-Carter, 1996; Singer and Kouda, 1997a and b; Raines, 1999; Harris *et al.*, 2001; Brown *et al.*, 2000; D'Ercole *et al.*, 2000; de Araujo and Macedo, 2002; Porwal *et al.*, 2003a and b). Many potential assessment studies based on georeferenced data integration were also published for various ore deposit models, namely:

- volcanogenic massive sulphide (VMS) deposits (Wright and Bonham-Carter, 1996; Dion and Lamothe, 2002; Lamothe *et al.*, 2005);
- orogenic gold deposits (Groves *et al.*, 2000; Knox-Robinson, 2000; Harris *et al.*, 2001; Rogge *et al.*, 2006; Lamothe and Harris, 2006; Lamothe, 2008);
- epithermal gold deposits (Boleneus *et al.*, 2001);
- Mississippi Valley-type deposits (D'Ercole *et al.*, 2000);
- Olympic Dam-Kiruna-type deposits (Lamothe and Beaumier, 2001 and 2002);
- kimberlite potential (Labbé, 2002; Paganelli *et al.*, 2002; Wilkinson *et al.*, 2006);
- porphyry Cu-Au-Mo deposits in the Abitibi (Carranza and Hale, 2002; Tangestani and Moore, 2003; Labbé *et al.*, 2006).

The production of a mineral potential map involves a series of steps (Figure 1). First, an appropriate exploration model (VMS, orogenic gold, etc.) must be selected for the targeted commodity or commodities. Based on the model, relevant geological parameters are selected and combined to create a **favourability** map. This initial step is critical because it allows the modeller to assess the availability of georeferenced data sources for each parameter, and as the case may be, to determine the amount of time required to acquire new sources of data. It is also during this step that an appropriate geodetic reference system and map projection will be chosen.

The second step consists in generating, for each selected parameter, a **digital evidential map** that will be integrated when processing the exploration model. The format of each map may be either binary (0 or 1), multiclass, or continuous (Harris *et al.*, 1999, 2000, 2001). This step of processing generally requires the use of spatial analysis or statistical processing software, often available as GIS extensions.

The third step of processing consists in integrating the various evidence maps to produce a favourability map. Integration methods are subdivided into two categories (Table 1): empirical or data-driven methods, and conceptual or knowledge-driven methods (see Bonham-Carter (1994) and Wright and Bonham-Carter (1996) for a detailed description). Empirical approaches require the presence, within the study area, of a sufficient number of deposits belonging to the targeted deposit model. These methods analyse spatial correlations between evidence data (parameters) and the location of known deposits, thus assigning a weight factor to each evidential map. Processing methods such as the Weight of Evidence method (WofE) (Bonham-Carter, 1994), logistic regression (Chung and Agterberg, 1980), and neural network analysis (Singer and Kouda, 1996 and 1999; Harris and Pan, 1999; Brown *et al.*, 2000) are all examples of this type of data-driven approach (Table 1).

Conceptual approaches harness the modeller's expertise to assign weight factors to evidential maps based on the exploration model. Although subjective, these methods make it possible to integrate in the processing the geologist's knowledge and experience. These methods include Boolean logic, multi-layer overlay (Harris, 1989), the Dempster-Schafer belief theory (Chung and Moon, 1991; An *et al.*, 1992) and fuzzy logic (An *et al.*, 1991).

It is possible to combine the two types of approaches to develop hybrid methods. For example, to assess the mineral potential for SEDEX-type deposits in India (Porwal *et al.*, 2003b) and for VMS-type or orogenic gold deposits in the Abitibi and Baie-James regions (Lamothe *et al.*, 2005; Lamothe and Harris, 2006; Lamothe, 2008), these authors used the Weight of Evidence method to weigh parameters, then converted these values into fuzzy weights and combined the evidential maps using a fuzzy logic approach (this is also the approach used in this study). In another example, Brown *et al.* (2003) used evidential maps weighed by fuzzy logic and combined them using neural networks to assess the mineral potential for orogenic gold deposits in Western Australia.

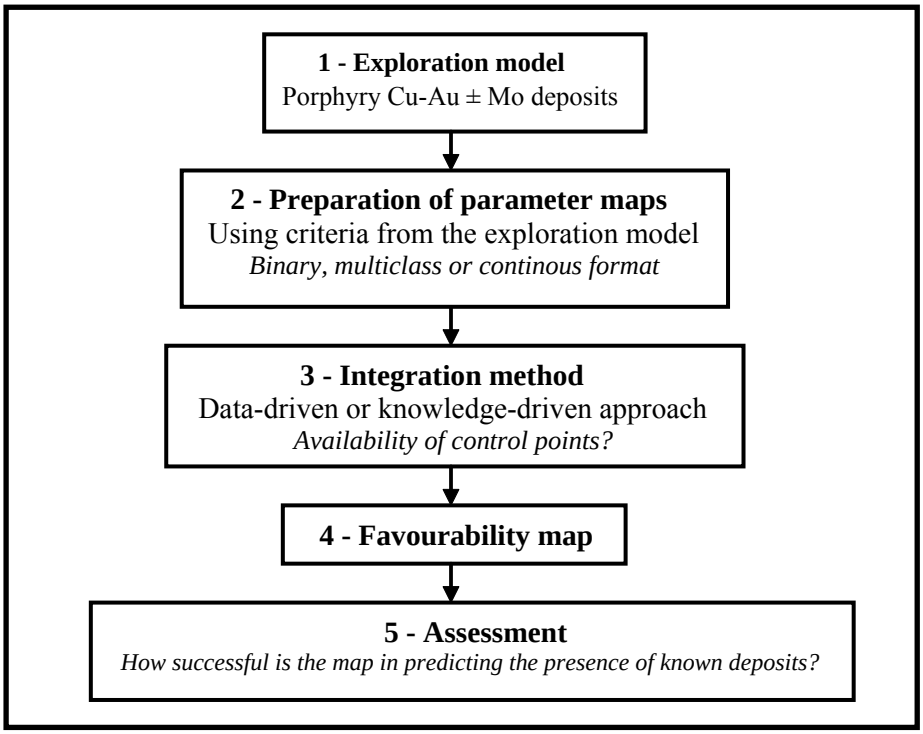

FIGURE 1 - Steps to create a favourability map through georeferenced data integration (modified from Harris *et al.*, 2006)

TABLE 1 – Methods to integrate evidential maps in a GIS environment.

Method	Processing	Combination criteria
Data-driven methods		
Weight of Evidence (WofE)	Control points (known deposits or occurrences)	Establish spatial correlations between known occurrences and tested variables (using Bayes' probability theorem)
Logistic regression	Control points (known deposits or occurrences)	Use spatial zones around known deposits to determine statistical criteria to apply to data layers in order to predict the presence or absence of mineral deposits
Neural networks	Control points (known deposits or occurrences)	Reproduce an anomalous set (i.e. mineral deposits) through a shape recognition process
Knowledge-driven methods		
Boolean operations	Geologist input	Sum of binary maps
Multi-layer overlay	Geologist input	Sum of weighed binary maps
Inference network and decision tree used in an expert system	Geologist input	
Dempster-Schafer belief theory	Geologist input	
Fuzzy logic	Geologist input	Assign to each indicator element map a fuzzy weight factor between 0 and 1; combine maps using fuzzy operators (and, or, gamma)
Analytic hierarchy process (AHP)	Geologist input	Sum of weighed favourability (continuous maps)

Favourability maps produced by the MRNF (Lamothe, 2008; Lamothe and Harris, 2006; Labbé *et al.*, 2006; Lamothe *et al.*, 2005) diverge from the vast majority of mineral potential assessment studies in two key aspects: 1) high-favourability zones are defined through the objective determination of a minimum favourability threshold; and 2) **targets** are defined based on unstaked portions of high-favourability zones (HFZ) at the time of the study (see section entitled "Determination of high-favourability zones and targets"). This type of target is by definition a temporary feature as it fluctuates according to the distribution of mining claims. It has nevertheless become an effective tool to promote mineral potential, as illustrated by the response of the mineral exploration industry each time a new potential assessment study is released. Since the addition in November 2007 of mineral potential maps and HFZ on GESTIM (the MRNF's web-based mining title management system), the concept of target has lost some of its relevance, but it still remains a valuable promotional tool.

The end result of the integration process is a georeferenced mineral potential map illustrating high-favourability zones for the targeted commodity. In addition to adequately predicting the presence of known deposits, this map should also reveal the existence of new exploration areas. The credibility of such a map lies with the effective measurement of favourability; counter-validation techniques are used to confirm the reliability of the selected processing method. This validation step is important, and whenever possible, should always be included in any serious potential assessment study.

Study objectives

The purpose of this study is to determine the location of high-favourability zones for porphyry-type Cu-Au ± Mo deposits in the Baie-James region (Figure 2). Among these zones, many of which are on currently staked lands, our work consists in defining a certain number of unstaked targets and to provide as much relevant data as possible to facilitate the assessment of each target. This approach allows members of the mining industry to quickly capitalize on the results of this study and allows the author to measure the impact of the study by documenting the number of targets staked following publication.

Another objective of this study is to establish the usefulness and credibility of this type of approach by measuring the favourability map's ability to predict, or predictivity, as well as its ability to recognize the presence of a validation set composed of porphyry deposits not used during processing.

General geology

The study area is primarily underlain by rocks of the Superior Province (Figure 3). It encompasses, from south to north, six major Archean geological subprovinces (Figure 4): 1) the **Abitibi Subprovince**, covering a narrow band along the southernmost part of the study area; 2) the **Opatica Subprovince**, in the south part of the area, mainly composed of gneissic plutonic rocks and metavolcanic rocks (Hocq, 1994); 3) the **Nemiscau Subprovince**, in the west part of the area, mainly composed of metasedimentary rocks (Card and Ciesielski, 1986); 4) the **Opinaca Subprovince**, composed of commonly migmatitic detrital metasedimentary rocks; 5) the **La Grande Subprovince**, a volcano-plutonic assemblage; and 6) the **Bienville Subprovince**, in the northwest corner of the area. The study area also contains outliers of Proterozoic sedimentary rocks of the Sakami Formation (north part of the area), the Mistassini and Otish basins, as well as parautochthonous units of the Timiskaming terrain in the Grenville Province, in the southeast corner of the area.

With rare exceptions, the vast majority of known porphyry deposits in the area are associated with volcanic belts in the La Grande and Opatica subprovinces (Figure 4) (Gauthier *et al.*, 1997; Gauthier and Laroque, 1998). La Grande rocks are comparable to those in the Sachigo-Uchi-Wabigoon subprovinces of northwestern Ontario (Goutier *et al.*, 2002). The La Grande Subprovince comprises two volcanic belts (Figure 3): 1) the **La Grande volcanic belt**, located in the north part of the subprovince, and comprising two volcanic cycles with distinct ages (Yasinski Group: 2736 +8/-6 Ma versus Guyer Group: 2820.3 ±0.8 Ma) and distinct lithological assemblages (Yasinski: basalts to rhyolites without komatiites versus Guyer: komatiites, basalts and felsic tuffs) (Goutier *et al.*, 2002); and 2) the **Middle and Lower Eastmain greenstone belt**, located in the south part of the La Grande Subprovince and comprising four volcanic cycles (cycle 1: 2752-2739 Ma; cycle 2: 2739-2720 Ma; cycle 3: 2720-2705 Ma; and cycle 4: <2705 Ma) (Moukhsil *et al.*, 2003).

The Opatica Subprovince is bounded to the north by the Nemiscau and Opinaca subprovinces, whereas its southern contact with the Abitibi Subprovince represents a major crustal suture zone defined by a north-verging fossil subduction zone (Calvert *et al.*, 1995). The Opatica is mainly com-

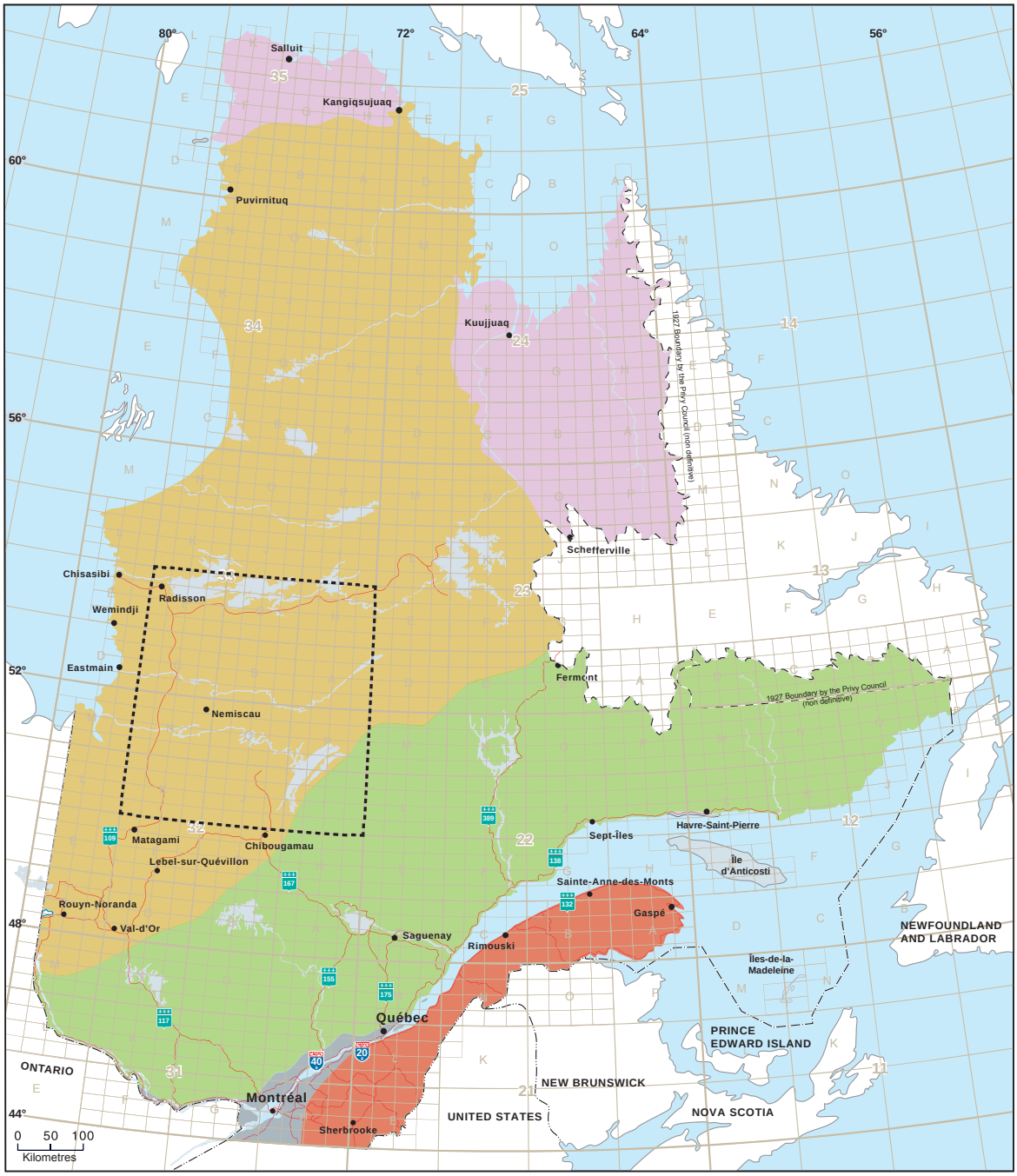

FIGURE 2 - Location of study area.

posed of thrust sheets dominated by an assemblage of locally migmatitic orthogneisses and syn- to late-tectonic plutons, among which Sawyer and Benn (1993) recognized five lithological suites with distinct ages. The **Frotet-Evans volcano-sedimentary belt** (FEVB) forms the top-lying thrust sheet overlying the structural assemblage in the Opatica (Sawyer and Benn, 1993). It is divided into four lithotectonic segments, including two volcanic-dominated segments at the eastern and western extremities (Frotet-Troilus and Evans-Ouagama segments), and two volcano-sedimentary segments in the centre (Storm-Evans and Assinica segments). U-Pb zircon analyses from felsic dykes associated with the porphyry Cu-Au deposit in the Frotet-Troilus segment yielded an age of 2782 ±6 Ma (Pilote *et al.*, 1997).

The metamorphic grade in the La Grande Subprovince ranges from the greenschist facies to the upper amphibolite facies, whereas rocks in the Opatica Subprovince are essentially upper amphibolite to granulite facies (Figure 5).

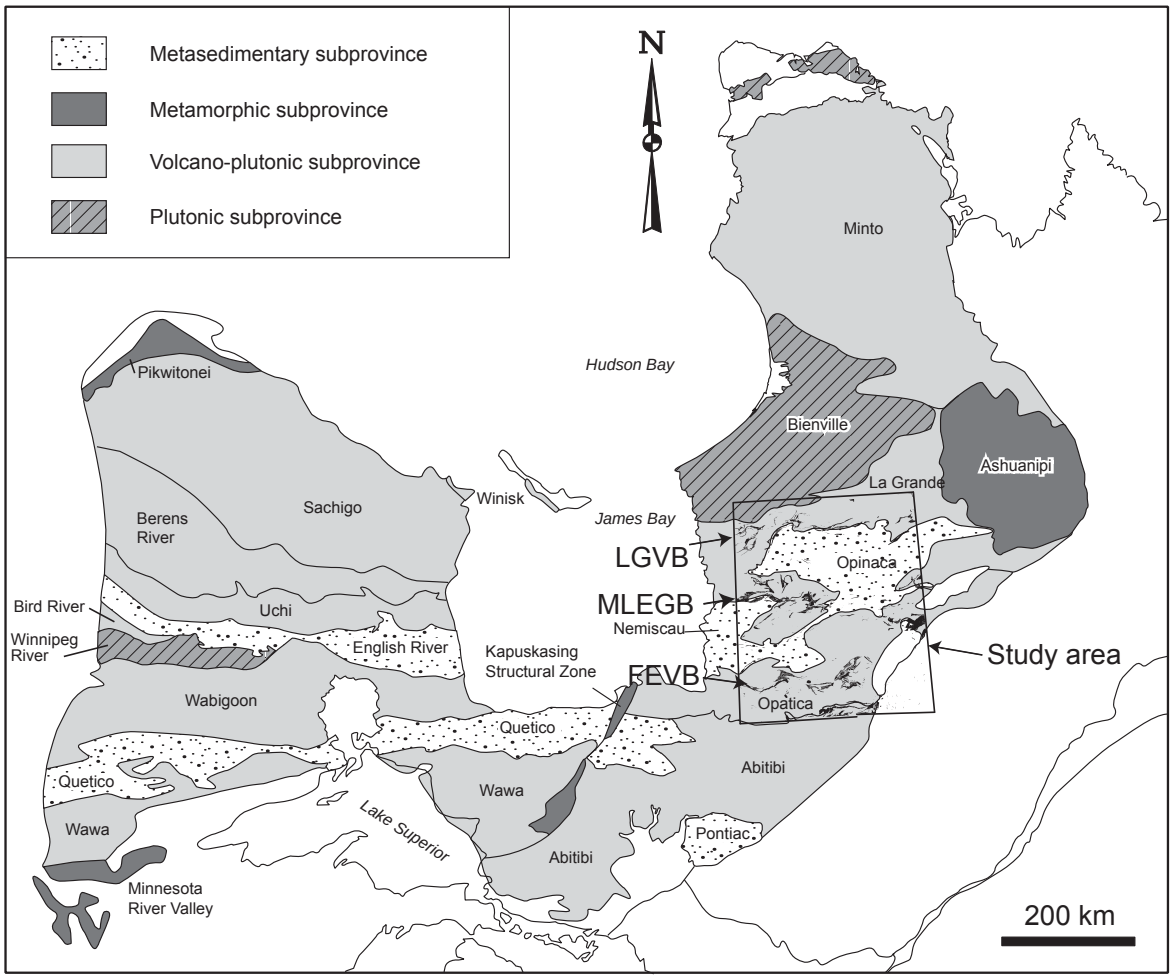

FIGURE 3 - Map showing the main subdivisions of the Superior geological Province. The base map is from Card and Ciesielski (1986) and Thurston (1991), subsequently modified by Goutier *et al.* (2002).
FEVB = Frotet-Evans volcanic belt; MLEGB = Middle and Lower Eastmain greenstone belt; LGVB = La Grande volcanic belt.

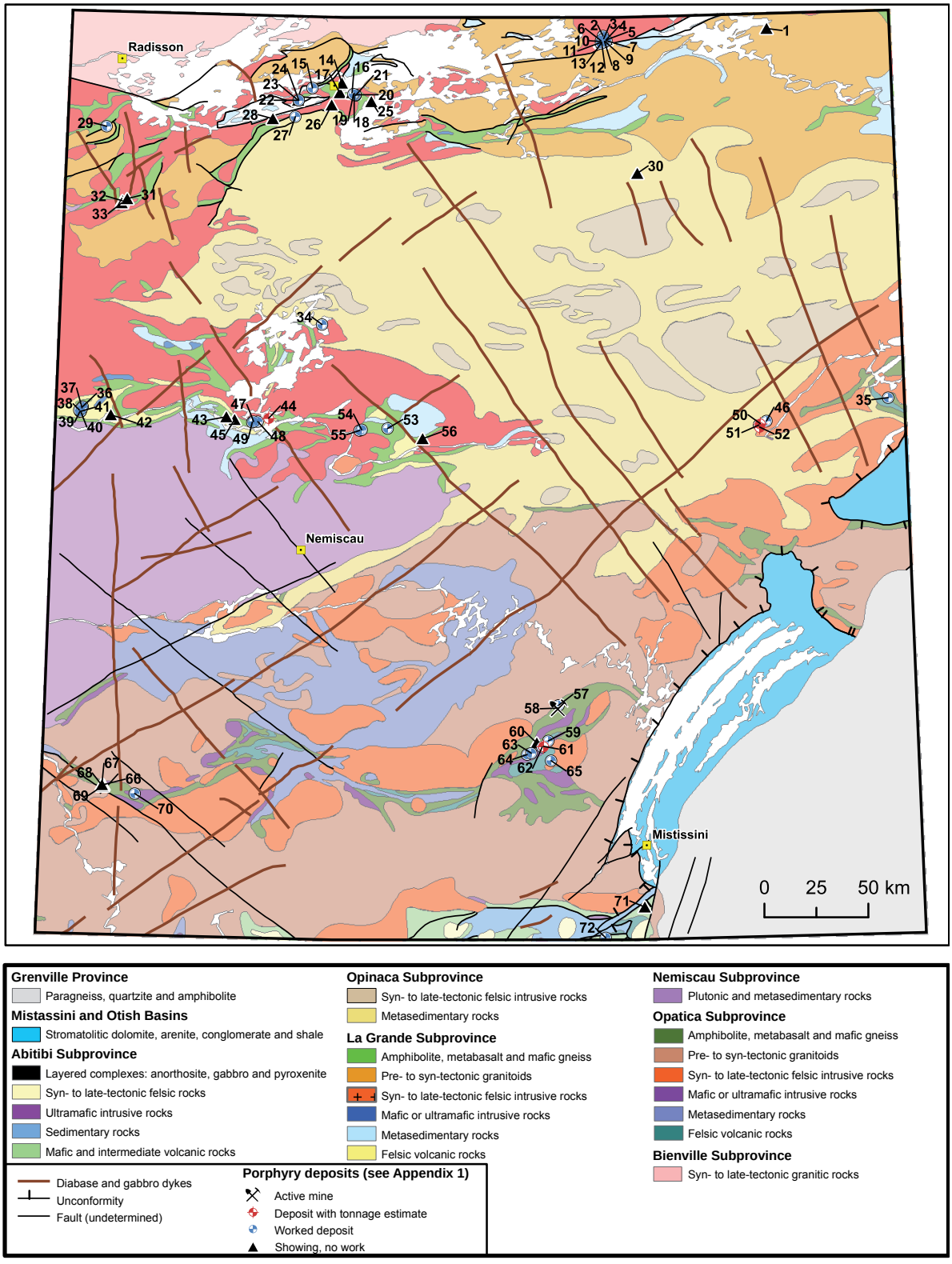

FIGURE 4 - General geology of the study area and location of porphyry deposits used in processing. Modified from Thériault (2002).

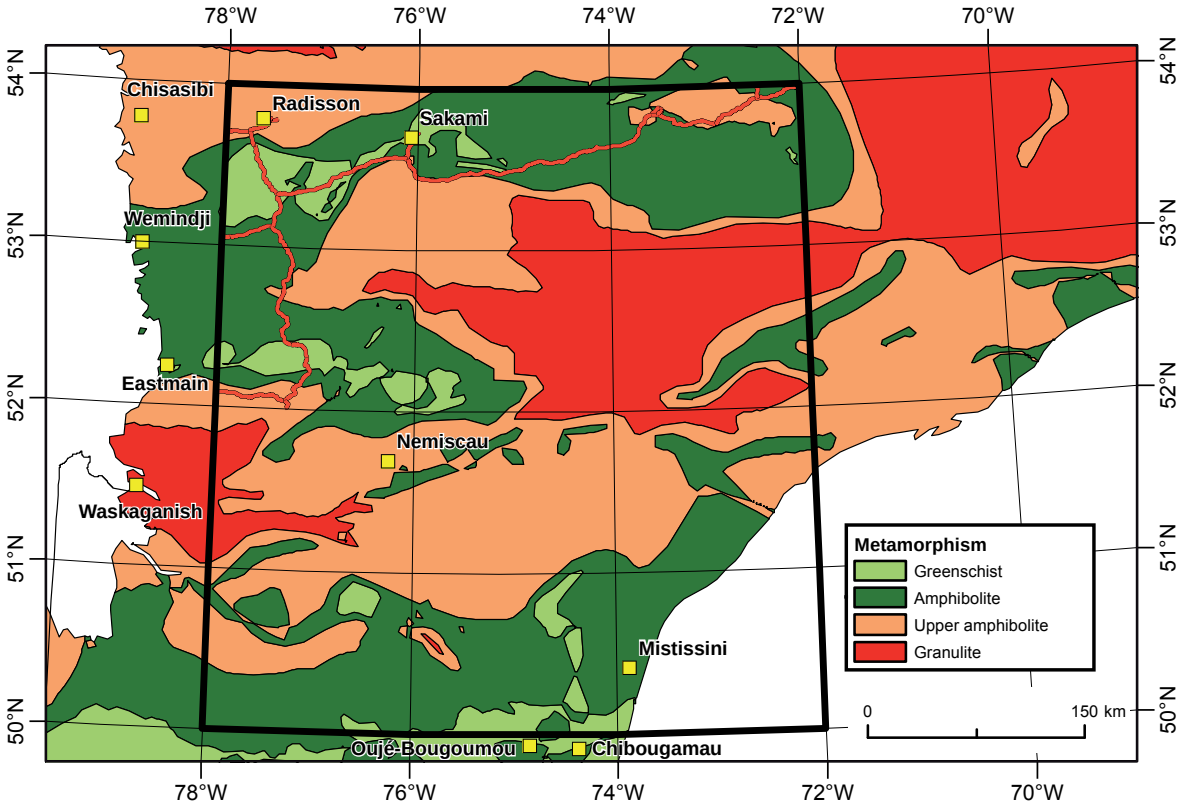

FIGURE 5 - Metamorphic map of the Baie-James region (Gauthier *et al.*, 2007).

METHODOLOGY FOR ASSESSING FAVOURABILITY

Introduction

Processing methods to assess mineral potential fall in one of two broad categories (Table 1): 1) empirical or data-driven methods, based on the analysis of spatial correlations between known mineral occurrences and certain geological parameters; the best known empirical methods are the Weight of Evidence (WofE) method and neural network analysis; and 2) conceptual or knowledge-driven methods, generally used in the absence of known deposits within the study area, that are based on the input of a geologist to assign a relative weight to each parameter. Among these methods, fuzzy logic is by far the most commonly used, mainly due to its flexibility and its simplicity.

Hybrid approaches combining the flexibility of knowledge-driven approaches with the rigour of data-driven approaches have recently been proposed (Brown *et al.*, 2003; Porwal *et al.*, 2003b). One of these, known as "hybrid fuzzy logic", can be used to get around one of the main difficulties encountered with the WofE method: the assumption underlying Bayes' Theorem that all of the data used (parameters) must be independent from one another. This condition is almost always violated when the method is applied in a geological setting, since many different categories of data are directly or indirectly based on one of the sources of evidence also used in modelling (for example contacts on a geological map interpreted from the magnetic field map). Although the approach remains valid for each parameter individually, the failure to meet this conditional independence clause tends to generate values that are too high, such that, when intermediate favourability maps are combined, posterior probability (resulting favourability) cannot be adequately calculated. For this reason, it was deemed more appropriate to combine evidential maps weighed with the WofE method using a knowledge-driven approach, namely fuzzy logic (hence the expression "hybrid fuzzy logic").

This combination of data-driven and knowledge-driven approaches is particularly appropriate to assess the mineral potential for porphyry Cu-Au ± Mo deposits in the Baie-James region, where a large number of deposits of this type are present in the region, allowing us to: 1) empirically calculate the probability of spatial association of parameters deemed relevant for this type of deposit; and 2) to combine, using fuzzy logic, evidential maps generated in this fashion, thus circumventing the parameter independence clause.

The selected approach is derived from the work of Porwal *et al.* (2003b) who proposed two approaches based on the concept of fuzzy logic: 1) knowledge-driven fuzzy logic, relying on the modeller's judgment to assign a fuzzy favourability value; and 2) data-driven fuzzy logic, where the fuzzy favourability value is established based on computations of the probability of association by the Weight of Evidence method. This second approach seems to be the most appropriate to process the selected model for the following reasons:

- the Baie-James region hosts 72 known occurrences of porphyry-type deposits and Chibougamau-type copper-rich veins (most of which are well documented) permitting the use of a data-driven approach;
- the use of the Weight of Evidence method to calculate favourability eliminates the inherent subjectivity of a knowledge-driven approach to processing, where the modeller, based on his/her perception (sometimes erroneous) of the relevance of a parameter, assigns to the latter an arbitrary favourability value;
- if elements are unduly included in a set of objects (poorly defined geological bodies; uncertain fault locations, etc.) that constitute a parameter, the WofE contrast value calculated for spatial association will be lower that what would theoretically have been obtained. As such, the inclusion of foreign elements not associated with porphyry deposits will result in a dilution of the spatial association value and will ultimately generate a lower favourability value. **The method therefore possesses an inherent tendency to underestimate the true favourability of a parameter in the case of erroneous inclusions**. We consider that this property of the processing method adds to the credibility of the study as a tool to promote mineral potential.
- the fuzzy logic approach to assess favourability is the most flexible of all methods. The selection of various operators to combine the different parameters makes it possible to adequately reproduce the expert knowledge entailed in assessing mineral potential in exploration;
- although it is desirable, the fuzzy logic approach does not require (as is the case for the Weight of Evidence method) that the data used meet the conditional independence requirement.

Methodology

The WofE approach to assess mineral potential for VMS deposits was used by Wright and Bonham-Carter (1996), Reddy *et al.* (1991), and Agterberg (1989). The Weight of Evidence method was also used to assess the potential for orogenic gold deposits (Bonham-Carter *et al.*, 1988; Porwal and Hale, 2000; Harris *et al.*, 2001) and epithermal gold deposits (Turner, 1997; Carranza and Hale, 2000; Boleneus *et al.*, 2001), as well as for porphyry copper deposits (Carranza and Hale, 2002)[1].

This technique was developed by Spiegelhalter (1986) and applied to mineral exploration by Bonham-Carter *et al.* (1988), Harris *et al.* (1995), Wright (1996), Wright and Bonham-Carter (1996), and Raines (1999). According to this approach, a series of evidential maps derived from geophysical, geochemical, and geological data are combined to produce a favourability map using Bayesian statistics. The spatial association of each evidential map is calculated relative to the location of known deposits. A pair of weight factors, W+ and W-, is calculated based on the amount of overlap between known deposits and the various classes of the evidential map. If no particular association is observed between known mineral occurrences and the evidential map, then W+ = W- = 0. A positive value for W+ indicates a positive association between known deposits and the evidential map. The contrast value C (where C = [W+] - [W-]) represents the degree of spatial association between the evidential map and known occurrences. In this document, a high C value (*i.e.* C > 4) for a class of values in an evidential map (for example, the class of cells located less than 200 m from a fault) indicates a strong association between known porphyry Cu-Au ± Mo deposits and this particular class of values (Figure 6).

The hybrid fuzzy logic approach uses the Weight of Evidence method (see section entitled "Introduction") to calculate the **favourability value** (Vfavor) based on the contrast value (C) determined using the set of equations below (Porwal *et al.*, 2003b)[2]. Equation (1) is used if the contrast value is positive. If the contrast value is negative, then equation (2) is used. If the contrast value is nil, then both equations will yield a favourability value of 0.5.

Vfavor = 0.5 + (Cij / 2 x Cmax) if $0 \leq Cij \leq Cmax$ (1)
Vfavor = 0.5 - (Cij / 2 x Cmin) if $Cmin < Cij \leq 0$ (2)
Cij = contrast value of class j on evidential map i
Cmax = maximum contrast value for all evidential maps
Cmin = minimum contrast value for all evidential maps

This approach, fairly similar to the one used by Cheng and Agterberg (1999), applies the notion of **relative weighting of evidential maps** since it establishes the favourability value based on the complete set of maps and classes used[3]. For the porphyry Cu-Au ± Mo deposit model applied to the Baie-James region, values for C_{max} and C_{min} are respectively 8.327 and –6.043.

The various maps generated in processing this ore deposit model are combined using fuzzy operators, some of which are equivalent to Boolean operators. Operators used in this study are FUZZY-GAMMA and OR. The use of the OR operator generates as output the maximum favourability value observed on combined maps. The FUZZYGAMMA operator allows the modeller to emphasize the importance of overlap for certain favourable parameters by generating a **result higher than the maximum value of cells in combined maps**. The FUZZYGAMMA operator is modulated with a gamma factor F, the value of which (generally in the range 0.80 to 0.97) is determined by the modeller and is proportional to the desired amount of emphasis.

Abuse of the FUZZYGAMMA operator at various steps in the combination process may generate artificial overweighing in the final assessment, since the application of a high F factor tends to artificially boost favourable values. To avoid this pitfall, the different factors used for FUZZYGAMMA operators were calibrated so as to obtain, on the final map, a background value of about 0.5. With this approach, this value represents the middle ground between a favourable association (positive contrast) and an unfavourable lack of association (negative contrast).

---

1 The ArcSDM module, an extension of Arcview 3.x or ArcGIS9.x provided free of charge by Natural Resources Canada, can be used to calculate the different variables in the Weight of Evidence method. A list and a short definition of values calculated by the WofE method for each parameter are provided in Appendix 2.

2 Absent values (NoData) were replaced with favourability values of 0.001 to avoid propagation in the final result when the favourability maps are combined.

3 The result of this approach is that at least one of the classes of parameters will have a favourability value of 1, whereas at least one other class will have a value of 0. There is a drawback to this, in that it is not possible to generate an intermediate favourability map for a predictive map before going through the entire process for all the maps used in the model, since the calculated favourability value depends on the minimum and maximum contrast values calculated for the entire set of maps.

Exemple 1: Example 1: More points in parameter B (non-random distribution)

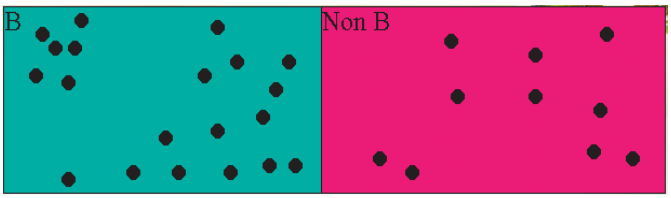

N(T) = 1000 cells (surface area of study area)
N(B) = 500 cells (surface area of parameter B)
N(Bpts) = 20 (number of points in parameter B)
N(D) = 30 (total number of control points)
W+ = 0.2980 W- = -0.4157 C = 0.7138

Exemple 2: Many more points in parameter B (non-random distribution)

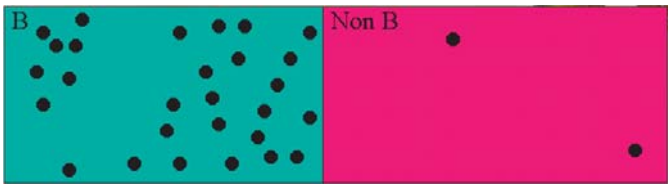

N(T) = 1000 cells (surface area of study area)
N(B) = 500 cells (surface area of parameter B)
N(Bpts) = 28 (number of points in parameter B)
N(D) = 30 (total number of control points)
W+ = 0.6513 W- = -2.0414 C = 2.6927

Exemple 3: Number of points in parameter B equal to random distribution

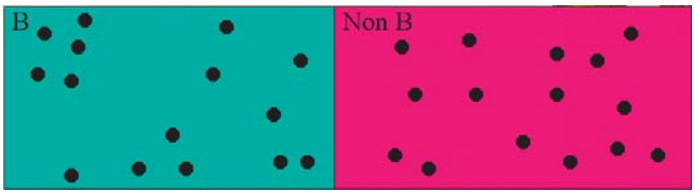

N(T) = 1000 cells (surface area of study area)
N(B) = 500 cells (surface area of parameter B)
N(Bpts) = 15 (number of points in parameter B)
N(D) = 30 (total number of control points)
W+ = 0.0 W- = -0.0 C = 0.0

FIGURE 6 - Examples of contrast value calculations based on the spatial association between control points and a parameter (modified from Bonham-Carter, training notes, Denver 2002).

The final result of the processing is a map of favourability values for porphyry Cu-Au ± Mo deposits. The process whereby the various parameters are integrated (the inference model) is illustrated in Appendix 3. Parameters are grouped into categories forming five sub-sets (see Table 2 in section 2.5): 1) presence of a heat source; 2) lithological control; 3) structural control; 4) hydrothermal activity; and 5) evidence in the secondary environment. Grouping into sub-sets makes it easier to understand the process and to interpret the results.

Characterization of porphyry-type deposits

Porphyry-type deposits represent one of the most important economic categories of non-ferrous metal deposits. These deposits are characterized by the presence of sulphide and oxide mineralization in veinlets and/or disseminations, within a large volume of hydrothermally altered rock (Seedorf *et al.*, 2005). Porphyry-type deposits worldwide are distributed in magmatic belts and are genetically related to intermediate to felsic epizonal to mesozonal intrusions, commonly referred to as porphyries. Essentially due to the preservation of epizonal terrains, the vast majority of porphyry-type deposits

are Phanerozoic, although several examples of Archean and Proterozoic deposits, albeit more modest economically, are reported in Canada and in Fennoscandia (Gaál and Isohanni, 1979; Fraser, 1993; Kirkham and Sinclair, 1996).

The main economic characteristics of porphyry-type deposits are as follows (Kirkham and Sinclair, 1996; Titley, 1993; Labbé *et al.*, 2006):

- they represent targets on the order of 100 million tonnes;
- metal grades for the various commodities, although highly variable, are generally less than 1%;
- they constitute the most important resource in Cu, Mo, and Re worldwide, and a close second for Au, Ag, Sn, W, Pt, Pd, and Se. In recent years, porphyry gold deposits have in fact been recognized as a major mineral resource (Vila and Sillitoe, 1991);
- they represent more than 99% of the combined reserves and production in Mo, in Canada and around the world;
- they represent between 50 and 60% of worldwide Cu production;
- less than 50% of the Cu production in Canada comes from this type of deposit, however they host nearly 60% of Canadian reserves.

The main geological characteristics of porphyry deposits are as follows (Figure 7):

- mineralization is generally hosted in a stockwork of cm-scale to mm-scale veins forming a halo around cogenetic intrusions;
- the porphyry system is commonly associated with the development of hydrothermal, magmatic, mechanical, or structural breccias (Seedorf *et al.*, 2005);
- the presence of pre-existing faults or syngenetic faults channels the flow of hydrothermal and mineralizing fluids;
- the emplacement of mineralization is generally accompanied by widespread hydrothermal alteration of adjacent rocks;
- porphyry intrusions associated with mineralization are generally volumetrically small (<0.5 km³) and their emplacement generally takes place between 1 and 6 km below surface (Seedorf *et al.*, 2005);
- alteration patterns around porphyry deposits vary depending on the nature of hydrothermal fluids. If the latter are acidic, the initial progression begins with early potassic alteration (biotite ± orthoclase), followed by sericitic alteration (muscovite ± chlorite) then by argillic alteration. If fluids are only weakly acidic, alteration will evolve from a calcisodic alteration zone (albite-actinolite) to a propylitic alteration zone (albite-epidote-chlorite-carbonate).

In Québec, the Lac Doré mining camp in the Chibougamau area constitutes the best example of a magmatic-hydrothermal system associated with numerous porphyry Cu-Au ± Mo deposits. Labbé *et al.* (2006) provides a brief overview of the latter and a thorough description is available in Pilote *et al.* (1998).

Several significant porphyry Cu-Au ± Mo deposits are known in the Baie-James region. The most important is the one at the Troilus mine, mined by Inmet Mining Corporation, where the tonnage is estimated at 32 Mt grading 1.5 g/t Au and 0.2% Cu (Larouche, 2005). Other examples include the Mac-Leod Lake polymetallic deposit (Western Troy Capital Resources; 24.4 Mt at 0.53% Cu, 0.076% Mo, 0.05 g/t Au, and 4.0 g/t Ag), the Reservoir C-52 deposit (Eastmain Resources; >10 Mt at 0.65 g/t Au and 0.12% Cu) and the Pointe Richard deposit (Western Troy Capital Resources; 877,000 t at 0.84% Cu, 0.22% Mo, 0.59 g/t Au, and 16 g/t Ag).

A global set of 72 porphyry deposits comprising one active mine, four deposits with a tonnage estimate, 39 worked deposits, and 28 showings (Appendix 1) was used to weigh the spatial association of geological parameters. Within this set, 11 deposits were randomly extracted to create a validation set and set aside prior to processing. The 61 remaining deposits were used to weigh the spatial association of parameters.

Given the relatively low number of worked porphyry deposits or deposits with tonnage estimates, compared to orogenic gold deposits for instance, deposits categorized as unworked showings were used for weighing and validation purposes in this study. Previous potential assessment studies conducted by the author avoided using the latter type of deposit – by definition being poorly documented and sometimes of an uncertain nature – since it has been demonstrated that integrating showings in weighing sets tends to reduce the predictivity of processing regardless of the method used (Harris

et al., 2006). However, given the very extensive size of the area covered by data processing and the high local concentrations of other types of deposits, the addition of showings was deemed necessary to adequately calibrate parameters.

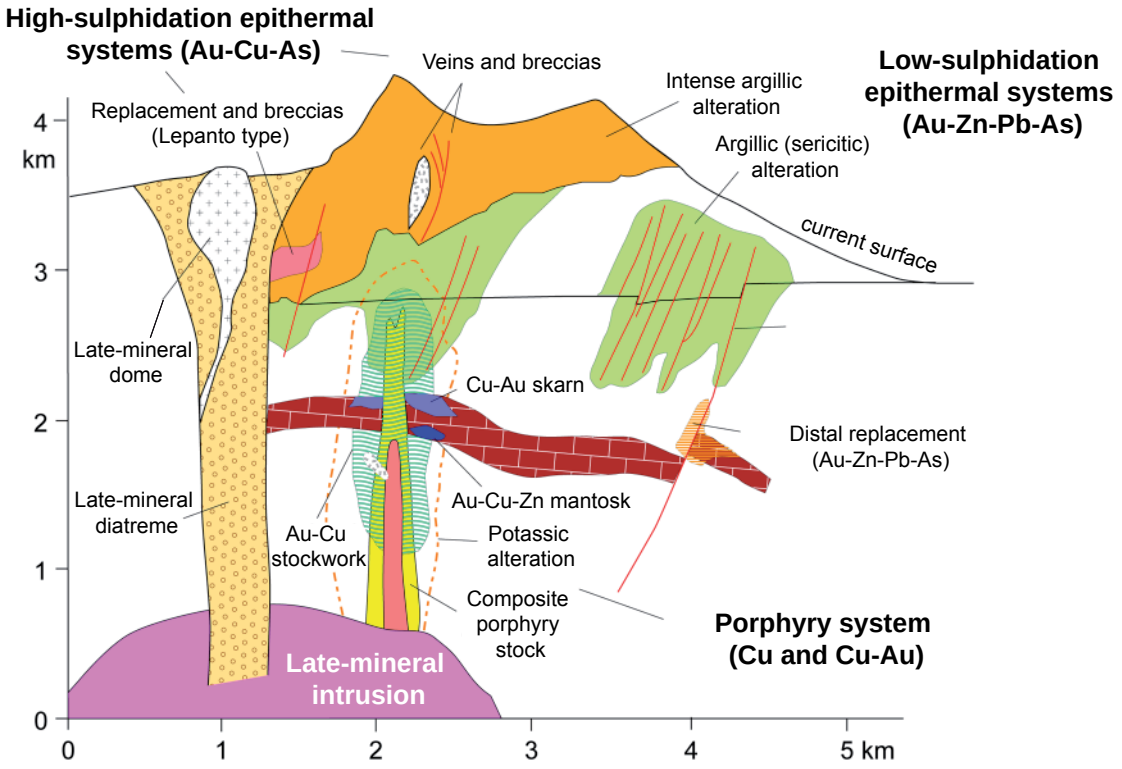

FIGURE 7 - Vertical cross-section illustrating various types of Cu-Pb-Zn-Ag-Au mineral deposit models potentially associated with a magmatic system in an andesitic volcanic setting; this type of setting occurs in the Western Pacific. A single magmatic system does not necessarily contain all the types of illustrated ore deposits, from porphyry-type to epithermal. Modified from Hollister (1985), Sillitoe (1989), and Kirkham and Sinclair (1996) (Source: Labbé *et al.*, 2006).

Level of knowledge within the study area

Figure 8 below illustrates the level of geological knowledge in the Baie-James region. It shows the density of documents, per 25-km² cell, extracted from the EXAMINE database. These documents were produced either by the MRNF or by mineral exploration companies. They namely include: 1) surface work such as geological surveys, statutory work reports, geophysical surveys, compilations, studies, and theses; and 2) point data such as drill holes and analytical results from rock samples or secondary environment samples.

Areas with a relatively high level of exploration (in orange or red) constitute the richest sources of relevant geological data for the potential assessment study relative to weakly explored areas (in blue). In the latter, processing is based on a limited number of useful elements in SIGÉOM, and the reliability of results is thus reduced. The true mineral potential of these areas may be underestimated by this processing.

Parameters used

The first step of any potential assessment study consists in selecting, among all the geological parameters coherent with the geological framework presented in section 2.3 and available in digital format for the study area, those that constitute effective indicators of the presence of porphyry Cu-Au ± Mo mineralization. To determine if this is the case, the Weight of Evidence method (Bonham-Carter *et al.*, 1989; Harris *et al.*, 2001; Lamothe *et al.*, 2005) was used to determine the spatial association of

each parameter with a set of 72 known porphyry-type deposits within the study area (see following section). Only those parameters that yielded a contrast value (C) above 1.5 were selected (Table 2). Some parameters that do not appear in Table 2 were tested but ultimately abandoned due to their low contrast value (namely competency contrasts, proximity to syn- and post-tectonic intrusions, proximity to tourmaline occurrences, chloritoid occurrences, and aluminosilicate minerals).

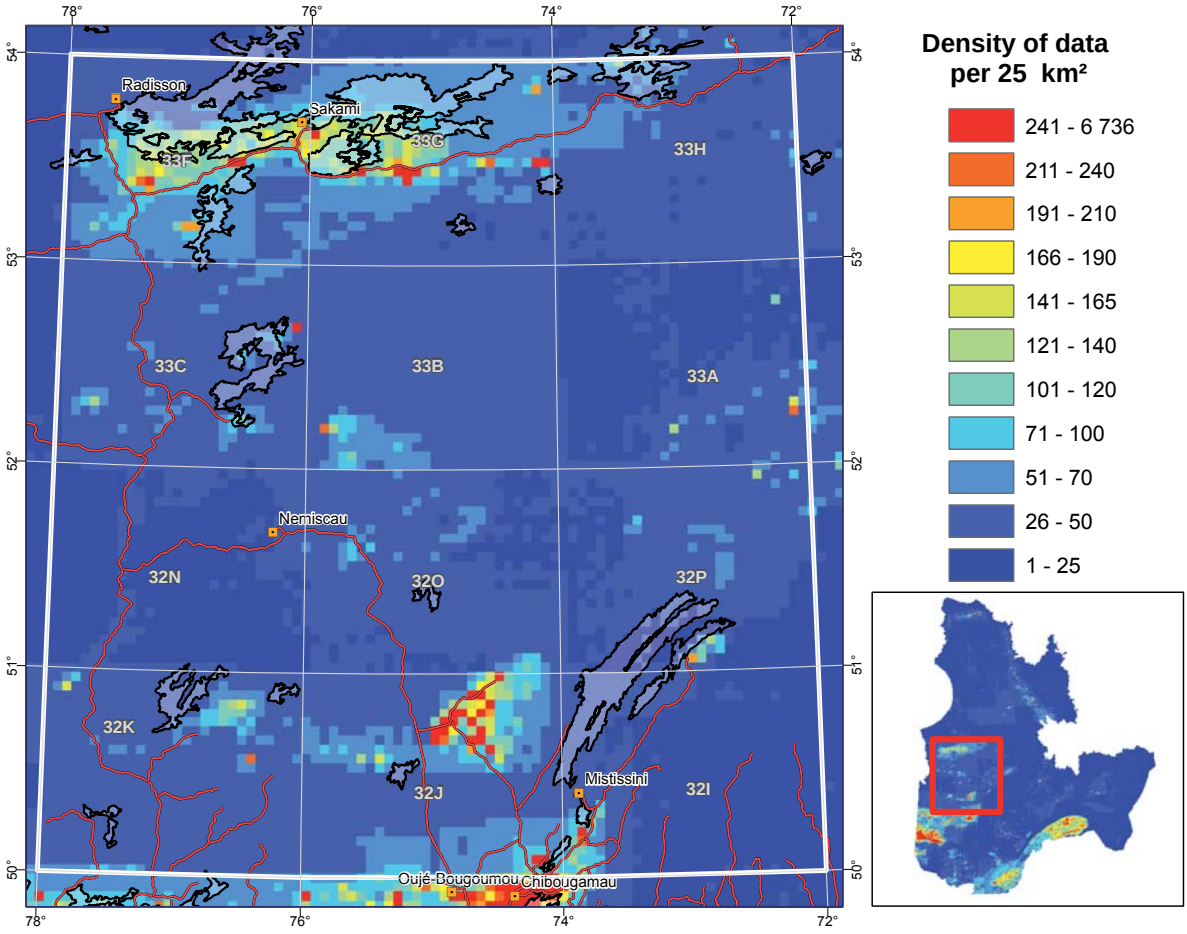

FIGURE 8 - Extract from the geological knowledge index map of Québec. Density calculations were performed using all available geological data in the province. The distribution of values in the legend is based on the natural breaks method (Jenks, 1967).

PROCESSING OF PARAMETER MAPS

Proximity to a heat source

The genesis of porphyry deposits requires a heat source able to generate and sustain hydrothermal activity through fluid convection in the country rock. As in Labbé *et al.* (2006), synvolcanic, syn- to late-tectonic, and post-tectonic intrusions were evaluated in the processing. However, only the first category showed a significant association with deposits in the weighing set (Appendix 2) and was thus subsequently kept for the modelling.

Proximity to a synvolcanic intrusion

The relatively minor amount of mapping and the lack of geochronology data over extensive parts of the study area are such that only a few synvolcanic intrusions were defined (Figure 9). The large

TABLE 2 - Parameters used to assess the mineral potential for porphyry Cu-Au ± Mo deposits in the Baie-James region. All digital data for individual parameters, combined maps and the final assessment map can be downloaded from the table by clicking on the appropriate hyperlink. Data are available in SHP and GRD (ESRI) format.

Parameter categories		Parameters used	Digital files	
Heat source		Proximity to a synvolcanic intrusion	SHP, GRD	**Favourability map for porphyry Cu-Au ± Mo deposits in the Baie-James region** PDF, GeoTIF, GRD
Lithological control GRD		Proximity to a felsic or intermediate porphyry intrusion	SHP, GRD	
		Proximity to a felsic or intermediate intrusion with hematite or magnetite	SHP, GRD	
Structural control GRD		Proximity to a regional ductile fault	SHP, GRD	
		Density of regional ductile faults	GRD	
		Density of faulting	GRD	
		Density of fracturing	GRD	
		Density of quartz veining	GRD	
		Proximity to a brecciated texture	SHP, GRD	
Hydrothermal activity GRD	**Analyses of indicator metals in the bedrock** GRD	Proximity to a copper anomaly ≥ 1000 ppm	SHP, GRD	
		Proximity to a gold anomaly ≥ 100 ppb	SHP, GRD	
		Proximity to a molybdenum anomaly ≥ 21 ppm	SHP, GRD	
		Proximity to a silver anomaly ≥ 3 ppm	SHP, GRD	
		Proximity to an arsenic anomaly ≥ 48 ppm	SHP, GRD	
		Proximity to a tungsten anomaly ≥ 5 ppm	SHP, GRD	
	Proximity to an anomalous NORMAT alteration index GRD	Proximity to an anomalous ISER index	SHP, GRD	
		Proximity to an anomalous ICHLO index	SHP, GRD	
	Proximity to an alteration indicator mineral GRD	Proximity to a potassic alteration indicator mineral	SHP, GRD	
		Proximity to a chloritic alteration indicator mineral	SHP, GRD	
		Proximity to an epidotization indicator mineral	SHP, GRD	
		Proximity to a silicification indicator mineral	SHP, GRD	
		Proximity to hematite or magnetite alteration	SHP, GRD	
	Proximity to sulphide or oxide mineralization GRD	Proximity to arsenopyrite mineralization	SHP, GRD	
		Proximity to bornite mineralization	SHP, GRD	
		Proximity to chalcopyrite mineralization	SHP, GRD	
		Proximity to magnetite mineralization	SHP, GRD	
		Proximity to molybdenite mineralization	SHP, GRD	
		Proximity to pyrite mineralization	SHP, GRD	
		Proximity to pyrrhotite mineralization	SHP, GRD	
	Secondary environment (lake-bottom sediments) GRD	Proximity to a copper anomaly	SHP, GRD	
		Proximity to a gold anomaly	SHP, GRD	
		Proximity to a molybdenum anomaly	SHP, GRD	

synvolcanic intrusions in the Eastmain area, between the 52nd and 53rd parallels, were taken from the regional compilation by Moukhsil *et al.* (2003). The small intrusion (La Grande Sud Tonalite) located south of Robert-Bourassa Reservoir and the group of intrusions near the Frotet-Troilus mine are based on work by Goutier *et al.* (2001) and Pilote *et al.* (1997) respectively.

Intrusions were buffered at 200-m intervals and contrast values were calculated with WofE. This step enabled us to determine that this parameter is predictive to a distance of 2,400 metres, and that it could be grouped into 4 distance classes (Appendix 2).

Due to the small number of mapped synvolcanic intrusions, several known porphyry Cu-Au ± Mo deposits show no spatial association with this parameter, which came in second to last (number 31) in terms of predictivity (Appendix 2).

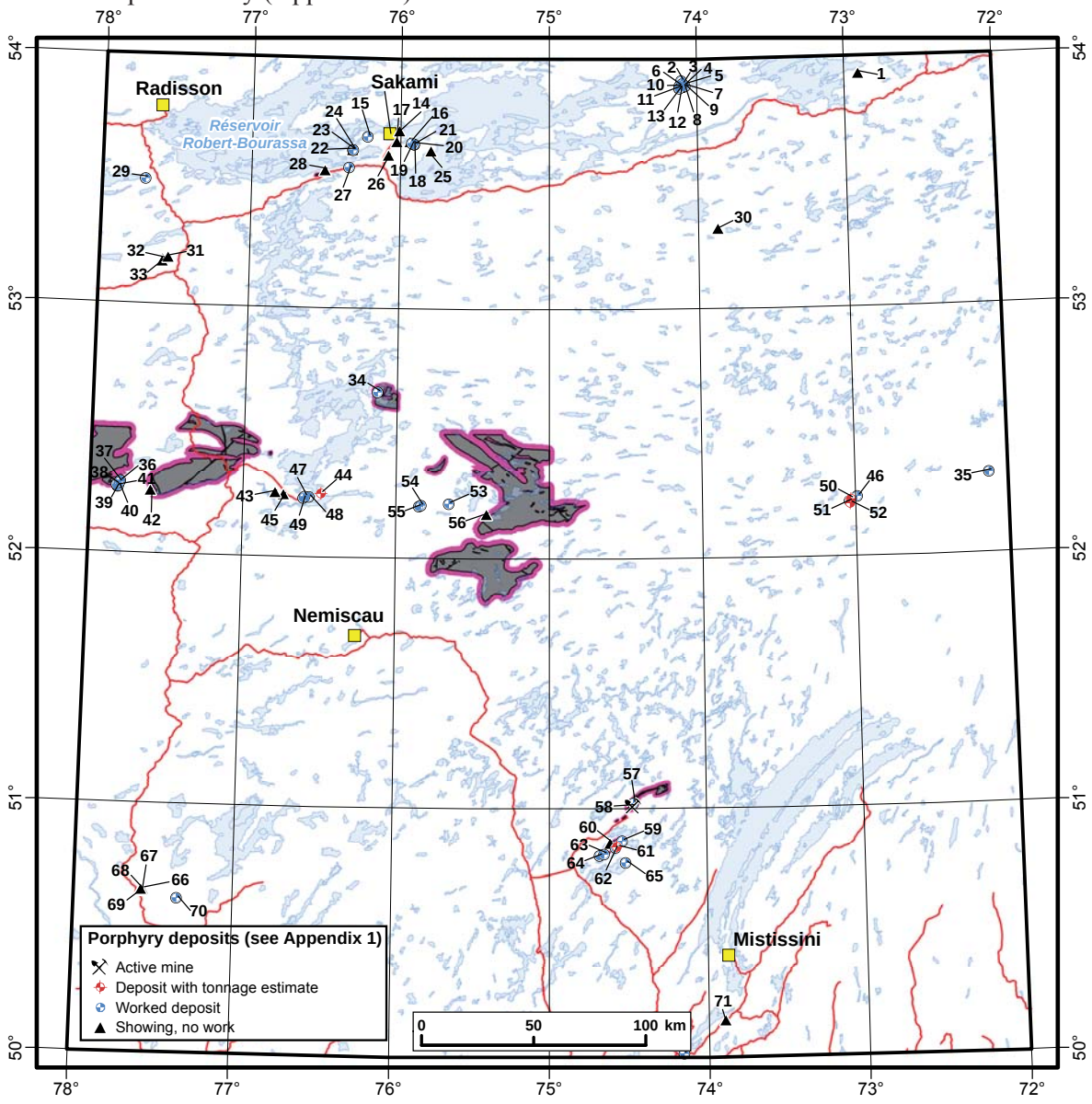

FIGURE 9 - Synvolcanic intrusions in the study area. The red outline corresponds to the 2,400-metre area of influence defined with WofE. See Appendix 1 for deposit identifications.

Lithological control

Two parameters were examined in this category: proximity to intermediate to felsic intrusions, either 1) porphyries, and/or 2) containing hematite or magnetite. A third parameter based on the relative competency of rocks, used by Labbé *et al.* (2006) in the Abitibi, was tested but rejected due to its low predictivity.

Proximity to a felsic or intermediate porphyry intrusion

Porphyry Cu-Au ± Mo deposits are commonly related to epizonal and mesozonal intrusions that are usually porphyritic and intermediate to felsic in composition. Lithological occurrences of these rock types can be processed as polygons extracted from geological maps, or as point occurrences extracted from field descriptions (*Géofiches*) or compilation outcrops (*compifiches*). The second approach proved to be more effective during processing, namely by reducing surfaces when calculating spatial association (the extensive surface area covered by geological polygons dilutes the probability of association in WofE) and by allowing the use of local observations that are sometimes too small to be included in maps.

Local observations were buffered at 200-m intervals and contrast values were calculated with WofE. This step enabled us to determine that this parameter is predictive to a distance of 600 metres and that it could be grouped into 4 distance classes (Appendix 2).

More than 15,700 local observations of intermediate to felsic intrusive lithologies are documented in the study area, most of which are probably related to syntectonic or post-tectonic plutons unrelated to porphyry deposits. Consequently, this parameter ranked 26th in terms of predictivity.

Proximity to a felsic or intermediate intrusion containing hematite and/or magnetite

The presence of hematite and/or magnetite is commonly observed in felsic intrusive rocks associated with porphyry-type mineralization (Seedorf *et al.*, 2005; Labbé *et al.*, 2006).

Hematite and/or magnetite observations in felsic or intermediate intrusive rocks were extracted from *géofiches* (2,474 occurrences), from compilation outcrop descriptions (83 occurrences) and from drill hole descriptions[1] (1,368 occurrences) within the study area. These combined observations were buffered at 200-m intervals and contrast values were calculated with WofE. This step enabled us to determine that this parameter is predictive to a distance of 1,200 metres and that it could be grouped into 4 distance classes (Appendix 2). The predictivity of this parameter is slightly better than the previous parameter, coming in at number 22. The presence, in intrusive rocks, of numerous magnetite occurrences related to high-grade metamorphism, which affects a large part of the area (Figure 5), contributes in reducing the effectiveness of this parameter.

Structural control

The emplacement of a major magmatic system typically associated with porphyry Cu-Au ± Mo deposits is, in most cases, accompanied by the construction of a volcanic edifice, generally andesitic in composition. A network of faults or stockworks accompanied by significant fracturing and brecciation develop in adjacent rocks throughout the evolution of the system, namely during the injection of magmatic-hydrothermal fluids (Burnham, 1979; Kirkham and Sinclair, 1996). This fracturing and brecciation channel fluid flow and promote adiabatic cooling of mineralizing fluids, leading to the precipitation of metal-rich minerals. Porphyry-type mineralization generally corresponds to veinlets and disseminations occurring in complex networks of mineralized fractures and breccia zones (Perry, 1961; Gilmour, 1977; Bushnell, 1988; Sillitoe, 1985).

Parameters in this category, detailed below, all illustrate at different degrees, this fundamental mechanical aspect of the ore deposit model. Some parameters that were tested but rejected due to their low predictivity include brittle lineaments, topographic lineaments, and presence of multiple dykes.

Proximity to a regional ductile fault

This processing step was conducted using a vector file of faults mapped throughout the area, from which Proterozoic faults preferentially oriented from N315° to N070° with no obvious geophysical expression were manually removed. Faults were buffered at 1,000-m intervals and contrast values were calculated with WofE. The parameter is predictive to a distance of 3,000 metres (Appendix 2) and ranks at number 30.

1 For all parameters used in this study, drill hole data are projected to the surface to calculate their spatial association with known deposits based on their actual location on surface.

Density of regional ductile faults

The spatial density of faults (number of faults per surface unit) constitutes an indicator of regional brittle deformation. A high density factor contributes in enhancing the circulation of hydrothermal solutions (Hagemann and Cassidy, 2000).

Using the file of mapped faults generated in the previous step, a raster image showing the density of faults per square kilometre within a 4,000-m radius was generated. Density values were regrouped into 10 classes using the natural breaks method of Jenk (1967). Optimization with WofE enabled us to determine that density values above 0.292 fault/km² are predictive. Two density classes were created and re-evaluated with WofE (Appendix 2). This parameter, much like the previous, appears to be one of the less predictive elements, coming in at number 29.

Density of faulting

This parameter corresponds to evidence of shearing or faulting observed in planar structures and noted in *géofiches* and drill hole descriptions (1,976 occurrences). Considering the fact that repeated observations within an area likely reflect a greater potential of hydrothermal circulation, this parameter was modelled in terms of density of observations.

Three density maps based on 1,000-m, 3,000-m, and 5,000-m radii were generated and regrouped using the method proposed by Jenk (1967). The predictivity assessment with WofE shows that density classes are more predictive when a 1,000-m radius is used. Density values were grouped into 5 density classes and re-evaluated with WofE (Appendix 2). This parameter is a good indicator of mineral potential, coming in at number 7 in the ranking.

Density of fracturing

Ore-forming processes in porphyry Cu-Au ± Mo systems are commonly associated with fracturing in the country rock. *Géofiches* and drill hole descriptions indicating evidence of fracturing in the rock (code FA) were extracted by query (342 occurrences). The parameter was tested with WofE in a first attempt, using a proximity criteria around fracturing observations, then in a second attempt using the density of observations per square kilometre. The second approach proved to be the best indicator (higher contrast) and was kept for the modelling. Three density classes were created above a minimum threshold of 0.32 fracture/km² (Appendix 2). At number 18, this parameter yields an average predictivity (0.819).

Density of quartz veining

About 68% of the descriptions for deposits used in the processing report the presence of quartz veins or pockets. Since the presence of quartz veins is not necessarily indicative of alteration in the rock, this parameter is considered as a structural indicator equivalent to fracturing in the rock.

Quartz vein observations were extracted from *géofiches*, compilation outcrop descriptions and drill hole descriptions[1]. As with the previous parameter, two approaches were tested with WofE, based either on the proximity to a point observation or on the density of observations/km². Once again the second approach proved to be the most effective indicator. Three density classes were created above a minimum threshold value of 0.01 vein/km² (Appendix 2). At number 13 in the ranking, this parameter is slightly above average in terms of predictivity.

Proximity to a brecciated texture

Porphyry-type deposits are commonly associated with the development of hydrothermal, magmatic, mechanical, or structural breccias (Sillitoe, 1985 and 1993; Seedorf *et al.*, 2005). Lithological descriptions corresponding to breccias or describing brecciated textures were extracted from *géofiches*, compilation outcrop descriptions and drill hole descriptions. Point occurrences were buffered at 200-m intervals and contrast values were calculated with WofE. The parameter, grouped into 3 classes, is predictive to a distance of 2,400 metres and ranks number 23 (Appendix 2).

1 Quartz vein descriptions in *géofiches* are fairly complex to extract in SIGÉOM. The presence of code I1N in the field "Rock Type" is the simplest case. To cover all possibilities, we also had to extract "Geological Units" with the code V or U and "Rock Types" with the code R or R1 or R1A or R1B or R1C or R1D or R2 or R3 or XXXX and the code QZ in the "Qualifier" or "Minerals" fields.

Evidence of hydrothermal activity in the bedrock

Country rocks around porphyry-type deposits are often hydrothermally altered and mineralized with sulphides and/or oxides. These alteration halos are generally large enough to constitute important indicators of regional or local proximity. Four main types of alteration are recognized in association with these deposits (Seedorf *et al.*, 2005): 1) alkali exchanges such as potassic alteration (biotite/sericite ± K-feldspar) or sodicalcic alteration (albite, actinolite, chlorite, epidote, titanite); 2) propylitic alteration (quartz, chlorite, epidote, calcite, and locally albite-pyrite); 3) hydrolytic alteration (sericitization, argillic alteration); and 4) silicification. The emplacement of mineralization is intimately linked with these alteration processes (generally with the potassic alteration phase) and for this reason, is processed in this section.

Indicator metal analyses

This sub-set of parameters groups metal indicators derived from lithochemical analyses available within the study area. These analyses are extracted either from geological surveys, from drill holes, or from statutory work reports. The 6 following metallic elements proved to be excellent predictors of the proximity of porphyry-type deposits. Copper, gold, and molybdenum were used by Labbé *et al.* (2006), whereas silver, arsenic and tungsten were added to the list of parameters in this study, as their predictivity was demonstrated in preliminary tests.

Proximity to a copper anomaly ≥ 1000 ppm

Processing was performed on 15,773 Cu analyses available throughout the area. As in Labbé *et al.* (2006), an arbitrary value of 1000 ppm (0.1%) was used as an anomalous threshold (1,470 occurrences). Anomalous samples were buffered at 200-m intervals and contrast values were calculated with WofE. This step enabled us to determine that the parameter is predictive to a distance of 1,600 metres and that it could be grouped into 5 distance classes (Appendix 2). As could be expected, this proximity indicator is one of the most effective, taking second place in the ranking.

Proximity to a gold anomaly ≥ 100 ppb

Processing was performed on 17,719 Au analyses available within the study area. The anomalous threshold for this element was arbitrarily set at 100 ppb (0.1 g/t) (Labbé *et al.*, 2006). The 2,859 selected occurrences were buffered at 200-m intervals and contrast values were calculated with WofE. This step enabled us to determine that this parameter is predictive to a distance of 2,400 metres and that it could be grouped into 5 distance classes (Appendix 2). This proximity indicator ranks sixth. The lower effectiveness (relative to copper) of this parameter may be explained by the presence of numerous orogenic gold deposits in the study area, that are totally unrelated to the current model. The presence of numerous gold analyses in a setting other than that for porphyry-type deposits contributes in diluting the predictivity of this indicator.

Proximity to a molybdenum anomaly ≥ 21 ppm

For molybdenum, the arbitrary threshold of 100 ppb set by Labbé *et al.* (2006) is probably too high to generate an effective indicator, considering the much lower number of analyses for this metal. To determine an appropriate threshold, a quantile-quantile diagram was created (Figure 10). According to the latter, a threshold of 21 ppm (point of departure from the reference line on the curve) is more appropriate. Anomalous samples (306 occurrences) were buffered at 200-m intervals and contrast values were calculated with WofE. This step enabled us to determine that this parameter is predictive to a distance of 1,600 metres and that it could be grouped into 4 distance classes (Appendix 2). This proximity indicator is the most effective in the entire set of parameters, taking first place in the ranking. This predictivity may be explained by the following: 1) molybdenum is only associated with the porphyry Cu-Au ± Mo deposit model considered here; and 2) this element is much more rarely analyzed than gold or copper, which avoided dilution when computing spatial association with WofE.

Proximity to a silver anomaly ≥ 3 ppm

The vast majority of porphyry-type deposits in the area show anomalous to very high silver grades. A quantile-quantile plot of 7,223 silver analyses from the study area shows that the anomalous threshold corresponds to 3 ppm (Figure 10). The 797 samples above this threshold were buffered at 200-m intervals and contrast values were calculated with WofE. This parameter is effective to a distance of 2,600 metres and comes in third place in terms of predictivity.

Proximity to an arsenic anomaly ≥ 48 ppm

Arsenic and its hosting mineral, arsenopyrite, are rarely documented in the description of porphyry-type deposits in the Baie-James region. However, As enrichment in many deposits, namely in British Columbia, in China and in the Andes, is reported in the literature (Williams *et al.*, 1999; Williams-Jones and Heinrich, 2005).

A quantile-quantile plot of 5,930 arsenic analyses within the study area shows that the anomalous threshold corresponds to 48 ppm (Figure 10). The 1,299 samples above this threshold were buffered at 200-m intervals and contrast values were calculated with WofE. This parameter is effective to a distance of 2,600 metres and ranks eleventh in terms of its predictivity.

Proximity to a tungsten anomaly ≥ 5 ppm

Porphyritic magmas associated with the genesis of molybdenum-rich deposits are generally less oxidized and contain lower S_{total} than those associated with copper-rich or gold-rich deposits (Seedorf *et al.*, 2005). These magmas commonly show elevated tungsten values. This element could therefore constitute a potential indicator for this ore deposit model.

The quantile-quantile plot for tungsten (1,685 analyses) shown in Figure 10 indicates that the anomalous threshold for tungsten should be 5 ppm. The 478 selected samples were buffered at 200-m intervals and contrast values were calculated with WofE. This parameter is effective to a distance of 2,400 metres and comes in ninth place in terms of its predictivity.

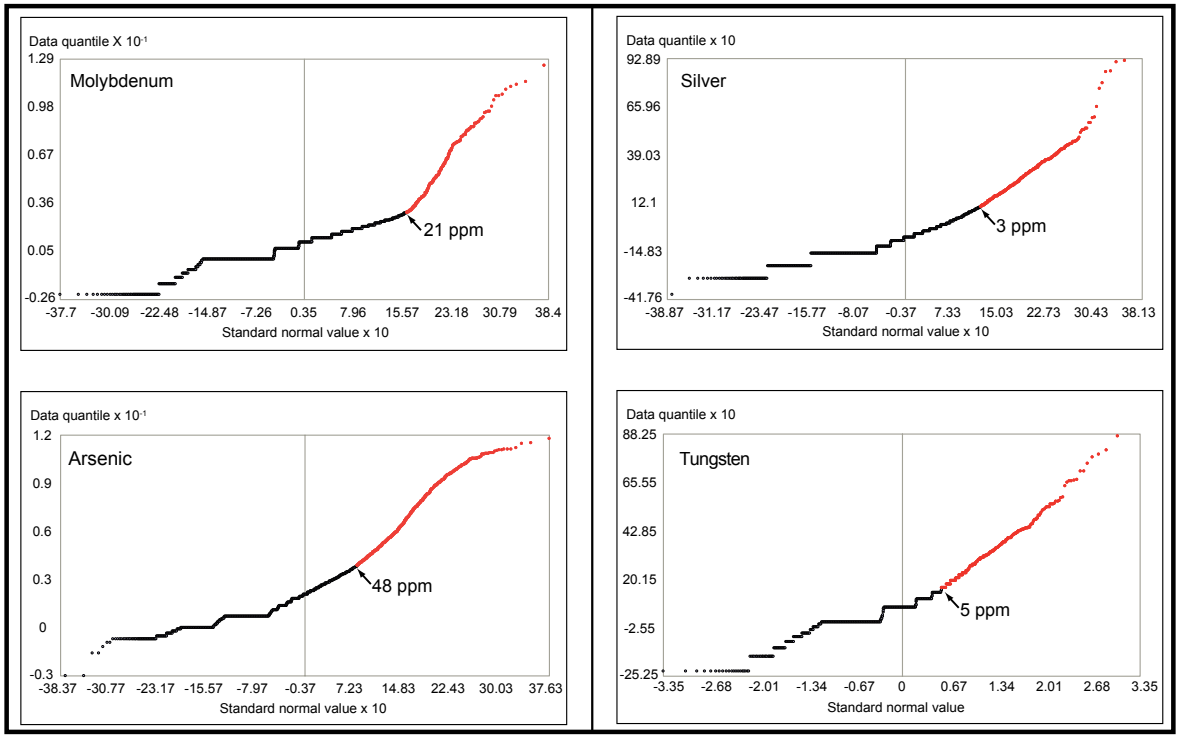

FIGURE 10 - Quantile-quantile plots showing anomalous thresholds for molybdenum, silver, arsenic, and tungsten. Selected samples appear in red on the curve.

Proximity to an alteration indicator mineral

Porphyry deposits are generally associated with voluminous alteration halos where mineralogical phases compose proximal to distal assemblages. Based on the 4 alteration processes mentioned in section 3.4 and depending on the nature of affected rocks, the five mineralogical indicators described below were defined. Each parameter was processed based on local occurrences (*géofiches*, compilation outcrop descriptions and drill hole descriptions) of one or more minerals specifically associated with each indicator. In addition to the different minerals mentioned below, tests were conducted to determine the predictivity of chloritoid and tourmaline observations, but the latter yielded inconclusive results.

Proximity to a potassic alteration indicator mineral

Géofiches, compilation outcrop descriptions and drill hole descriptions mentioning muscovite, sericite, or biotite alteration were extracted by query (4,661 occurrences). Distance buffers at 200-m intervals were created and optimized into 5 distance classes with WofE (Appendix 2). This parameter is effective to a distance of 3,400 metres and ranks number 14 in terms of predictivity.

Proximity to a chloritic alteration indicator mineral

Targeted minerals indicative of chloritic alteration are chlorite and amphibole (hornblende, anthophyllite, actinolite, grunerite or riebeckite). The 13,493 point occurrences thus obtained were buffered at 200-m intervals and contrast values were calculated and optimized into 4 distance classes with WofE (Appendix 2). This parameter is effective to a distance of 1,000 metres and ranks 21st in terms of its predictivity.

Proximity to an epidotization indicator mineral

Descriptions of epidote alteration (including pistachite or clinozoisite) were extracted (3,663 occurrences) and buffered at 200-m intervals. Following optimization with WofE, 5 distance classes were created (Appendix 2). The parameter is valid to a distance of 2,800 metres and ranks 20th.

Proximity to a silicification indicator mineral

The 779 occurrences (mainly derived from drill hole descriptions) that mentioned evidence of silicification were buffered at 200-m intervals and contrast values were calculated and optimized into 4 distance classes with WofE (Appendix 2). This parameter is effective to a distance of 2,600 metres and comes in 8th place in terms of predictivity.

Proximity to hematite or magnetite alteration

The addition of hydrothermal iron (magnetite or hematite) is typical of certain deposits (Sillitoe, 1993). Some 3,207 occurrences were extracted, buffered, and optimized into 4 distance classes with WofE (Appendix 2). This parameter is valid to a distance of 1,200 metres and its predictivity takes 10th place in the ranking.

Proximity to an anomalous NORMAT alteration index

Evidence of hydrothermal activity may translate into the presence of anomalous concentrations of normative minerals in igneous rock analyses. To this end, normative mineral indices ISER and ICHLO were calculated using NORMAT software and used to quantify alteration regardless of the original composition of the rock (Piché and Jébrak, 2004). These computations were conducted on a database of 17,047 major element analyses consisting of intrusive or effusive rock samples.

Proximity to an anomalous ISER index

A quantile-quantile plot was constructed with all 4,539 analyses that yielded a non-nil ISER index. The anomalous threshold determined in this fashion corresponds to ISER values equal to or greater than 42% (Figure 11). The 645 selected samples were buffered at 200-m intervals and contrast values were calculated and optimized into 4 classes with WofE (Appendix 2). This parameter is effective to a distance of 1,800 metres and ranks 12th in terms of predictivity.

Proximity to an anomalous ICHLO index

The procedure described above to determine the anomalous threshold for the ISER index was used for the 816 samples showing non-nil ICHLO index values (Figure 11). The threshold was set at 10% or more. The 631 selected samples were then buffered at 200-m intervals and contrast values were calculated and optimized into 4 classes with WofE (Appendix 2). This parameter is effective to a distance of 2,400 metres and its predictivity comes in at number 19 in the ranking.

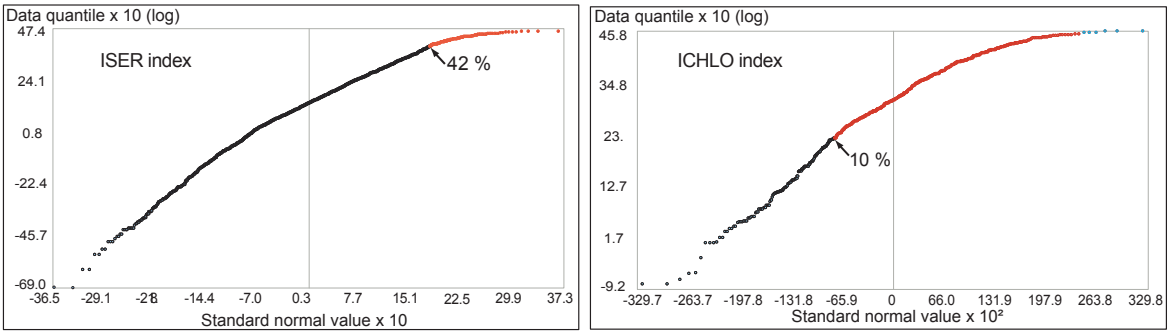

FIGURE 11 - Quantile-quantile plots for normative indices ISER and ICHLO calculated using NORMAT software (Piché and Jébrak, 2004). Anomalous thresholds are respectively 42% and 10%.

Proximity to sulphide or oxide mineralization

This sub-set of the model groups local observations of sulphide or oxide mineralization derived from *Géofiches*, compilation outcrop descriptions and drill hole descriptions in the study area. Targeted minerals include arsenopyrite, bornite, chalcopyrite, magnetite, molybdenite, pyrite, and pyrrhotite. All of these minerals are recognized, sometimes on their own but more commonly in polymineralic assemblages, in association with porphyry deposits (Seedorf *et al.*, 2005). For each indicator described below, point occurrences were buffered at 200-m intervals and contrast values were calculated and optimized into 4 classes with WofE (Appendix 2).

Proximity to arsenopyrite mineralization

Mineralogy descriptions indicating the presence of arsenopyrite in drill holes and *Géofiches* were extracted (225 occurrences). This parameter is effective to a distance of 7,800 metres and its predictivity comes in 17th place (Appendix 2).

Proximity to bornite mineralization

Only 15 bornite observations, essentially in *Géofiches*, were documented in SIGÉOM. This parameter is effective to a distance of 2,000 metres and its predictivity comes in fourth place (Appendix 2). This high level of predictivity can be explained largely by the limited number of observations and their frequent association with known porphyry deposits. The paucity of observations however, makes this parameter less useful in terms of locating new deposits.

Proximity to chalcopyrite mineralization

A total of 1,179 chalcopyrite observations are documented in SIGÉOM. This parameter is fairly proximal, as it remains predictive to a distance of only 1,000 metres. It ranks 5th in terms of its predictivity (Appendix 2). The large number of observations, its proximal association and its good predictivity make it a very effective parameter for this ore deposit model.

Proximity to magnetite mineralization

This parameter is based on all point observations of magnetite, regardless of the rock type. It is considered here as an accessory mineral, and not as an alteration mineral. The large number of occurrences (4,883 cases) confirms that this is a very common mineral and reflects in many cases the high metamorphic grade, which affects a large part of the study area. Despite this significant dilution factor, the parameter remains a valid predictor, at number 25 in the ranking (Appendix 2).

Proximity to molybdenite mineralization

The presence of molybdenite is rarely reported in *Géofiches* and drill hole descriptions within the study area (55 occurrences). The parameter is effective to a distance of 3,000 metres and comes in 24th place in terms of its predictivity (Appendix 2).

Proximity to pyrite mineralization

Pyrite is one of the most common sulphide phases and was reported in 3,469 different locations in *Géofiches* and drill hole descriptions. It is a very proximal indicator, generally observed within less than 600 metres from a porphyry deposit (Appendix 2). This parameter ranks 15th in terms of its predictivity.

Proximity to pyrrhotite mineralization

Similar to pyrite, the presence of pyrrhotite is commonly reported in the area (2,155 observations). It is not as proximal an indicator as pyrite is however; it is generally observed less than 1,600 metres away from a porphyry deposit (Appendix 2). This parameter comes in at number 16 in the ranking.

Evidence of mineralization in the secondary environment

The Baie-James area was almost entirely covered (Figure 12) by various sampling surveys for lake-bottom sediments (25,224 samples), stream sediments (19,023 samples), soils (4,373 samples) and tills (564 samples). Considering the homogenous distribution of lake-bottom sediment samples and the very high concentration of stream sediment samples south of Robert-Bourassa Reservoir, it was deemed preferable to only use stream sediment samples in areas not covered by lake-bottom sediment surveys (1,835 samples).

This part of the processing uses the same elements used as indicators by Labbé *et al.* (2006)[1]. For each type of survey, the anomalous threshold was determined using quantile-quantile plots (Figure 13). For comparative purposes, the corresponding percentile was indicated for each anomalous threshold thus defined (Table 3).

Proximity to a copper anomaly

Using quantile-quantile plots, anomalous thresholds were determined for copper analyses in samples of lake-bottom sediments (23,215 cases), stream sediments (1,835 cases), soils (4,375 cases) and tills (564 cases) (see Figure 13 and Table 3). The 441 anomalous samples extracted for the 4 types of sediments were buffered at 200-m intervals and contrast values were calculated and optimized into 3 classes with WofE (Appendix 2). This parameter is predictive to a distance of 2,600 metres and comes in 27th place.

1 The SIGÉOM database of lake-bottom sediment analyses in the Baie-James region is composed of samples from several different surveys with varying methodologies and analytical detection limits. For processing, a file of smoothed copper values created by CONSOREM was used for the three elements that are considered here (Cu, Au, Mo).

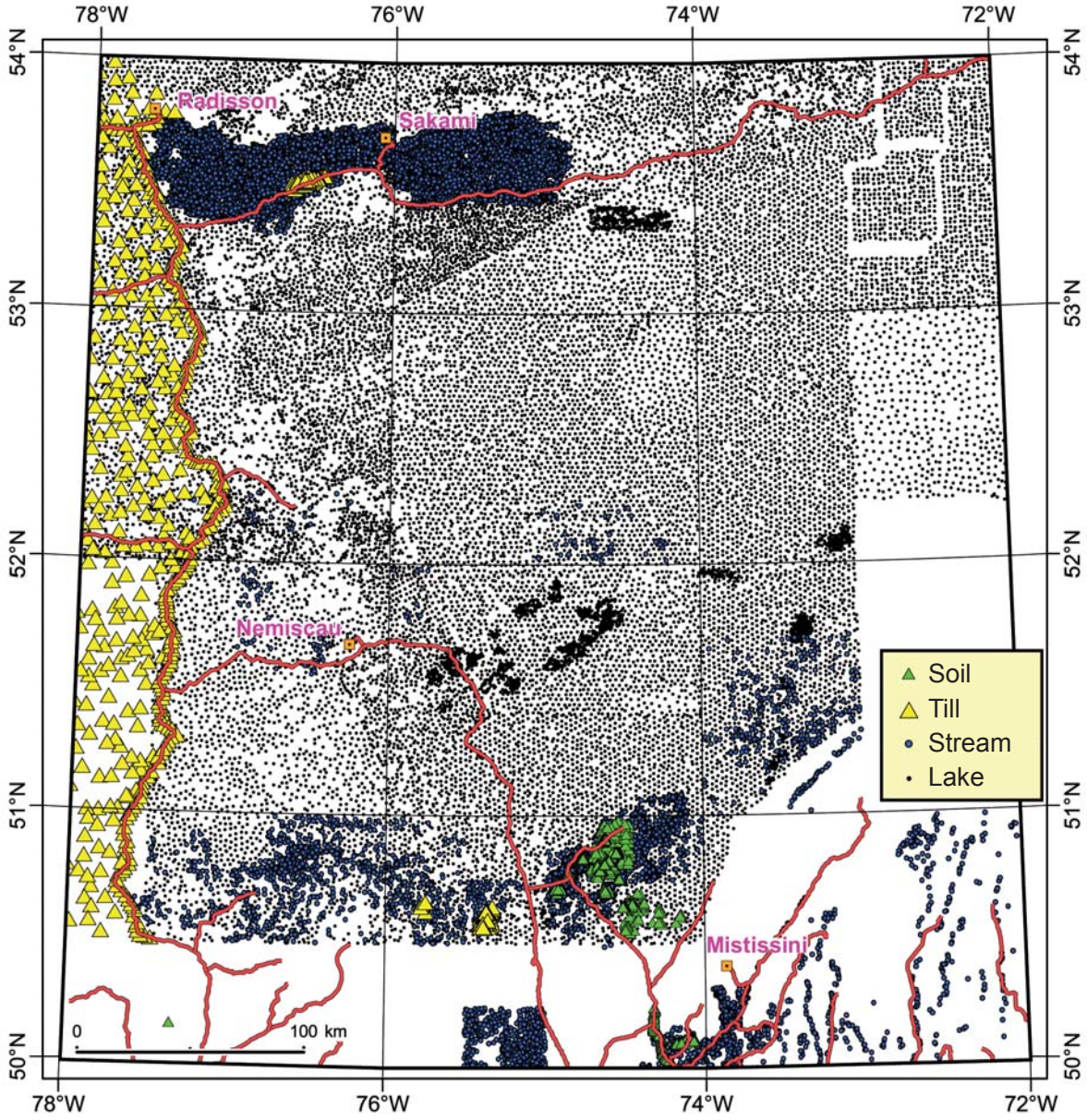

FIGURE 12 - Map illustrating the coverage for the various types of sampling surveys in the secondary environment used in processing.

TABLE 3 - Anomalous threshold values used for secondary environment indicators.

Sediment	Cu		Au		Mo	
	ppm (*percentile*)	# anom. samples	ppb (*percentile*)	# anom. samples	ppm (*percentile*)	# anom. samples
Lake	47 (*99*)	238	6 (*95*)	334	12 (*95*)	1139
Stream	40 (*94*)	106	16 (*98*)	23	6 (*95*)	564
Soil	65 (*99*)	50	16 (*97*)	79	6 (*98*)	100
Till	32 (*92*)	47	90 (*75*)	12	4 (*93*)	26
Total		441		448		1829

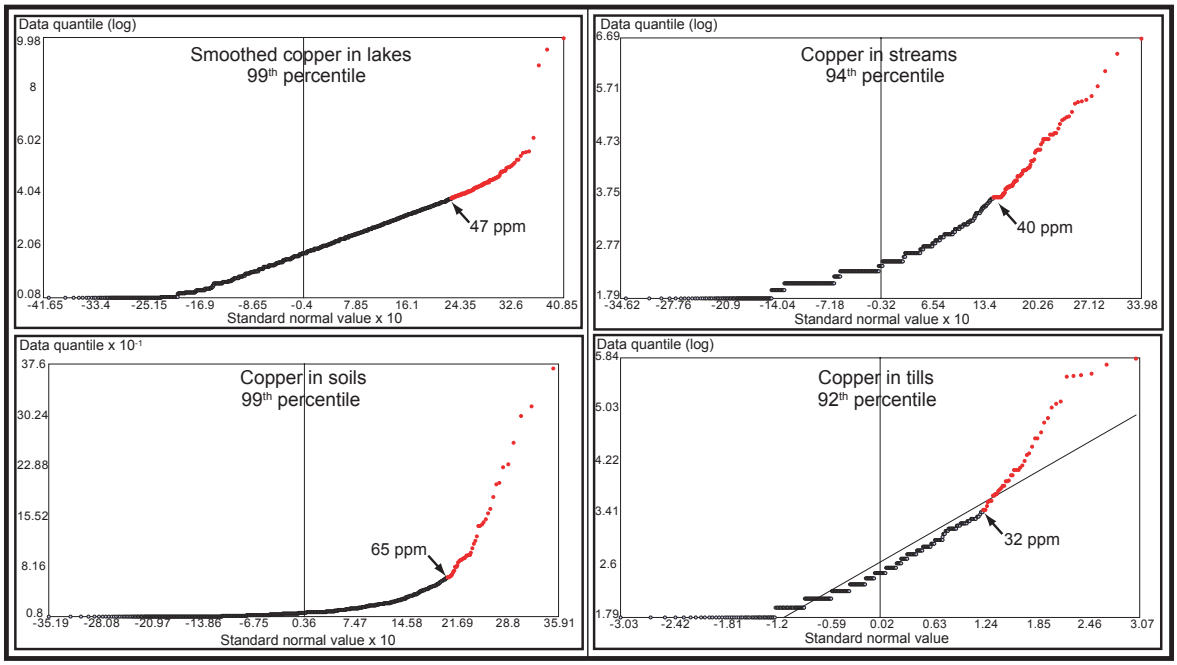

FIGURE 13 - Quantile-quantile plots used to define the anomalous threshold value for copper in lake-bottom sediments, stream sediments, soils, and tills in the Baie-James region.

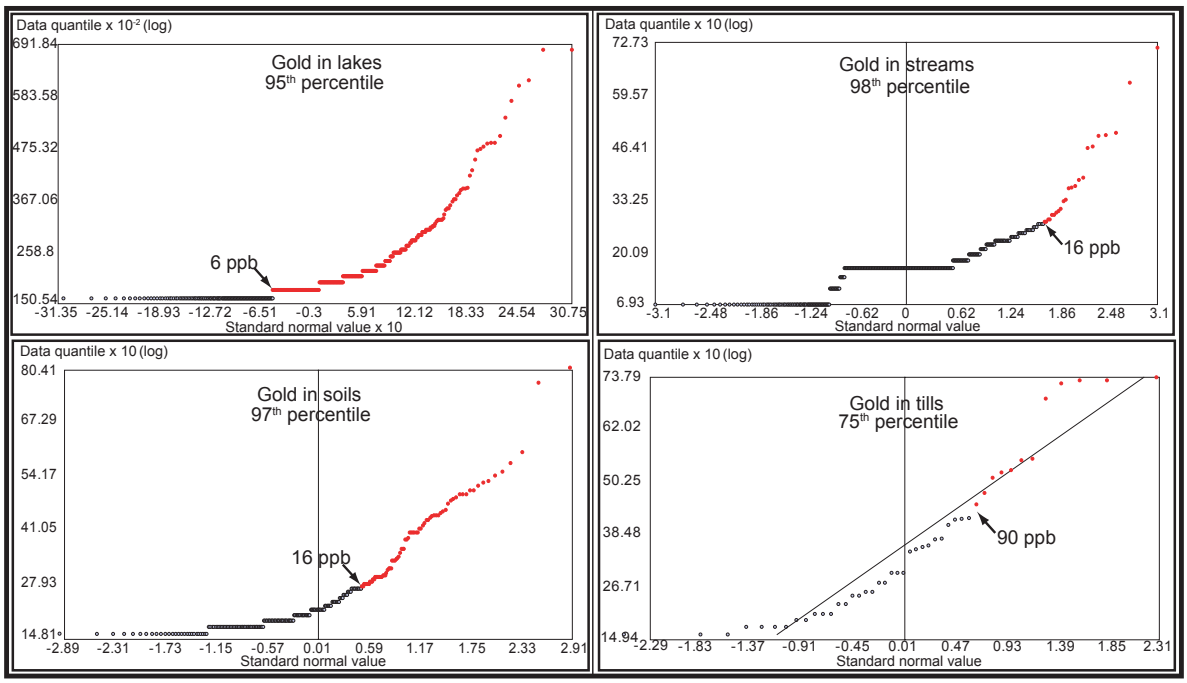

FIGURE 14 - Quantile-quantile plots used to define the anomalous threshold value for gold in lake-bottom sediments, stream sediments, soils, and tills in the Baie-James region.

Proximity to a gold anomaly

Using quantile-quantile plots, anomalous thresholds for gold analyses in samples of lake-bottom sediments (6,491 cases), stream sediments (973 cases), soils (2,987 cases), and tills (45 cases) were determined (Figure 14 and Table 3). The 448 anomalous samples extracted for the 4 types of sediments were buffered at 200-m intervals and contrast values were calculated and optimized into 4 classes with WofE (Appendix 2). This parameter is predictive to a distance of 3,200 metres and comes in 32nd place.

Proximity to a molybdenum anomaly

Using quantile-quantile plots, anomalous thresholds for molybdenum analyses in samples of lake-bottom sediments (23,159 cases), stream sediments (12,017 cases), soils (4,366 cases) and tills (344 cases) were determined (Figure 15; Table 3). The 1,829 anomalous samples extracted for the 4 types of sediments were buffered at 200-m intervals and contrast values were calculated and optimized into 3 classes with WofE (Appendix 2). The parameter is predictive to a distance of 1,400 metres and ranks in 28th place.

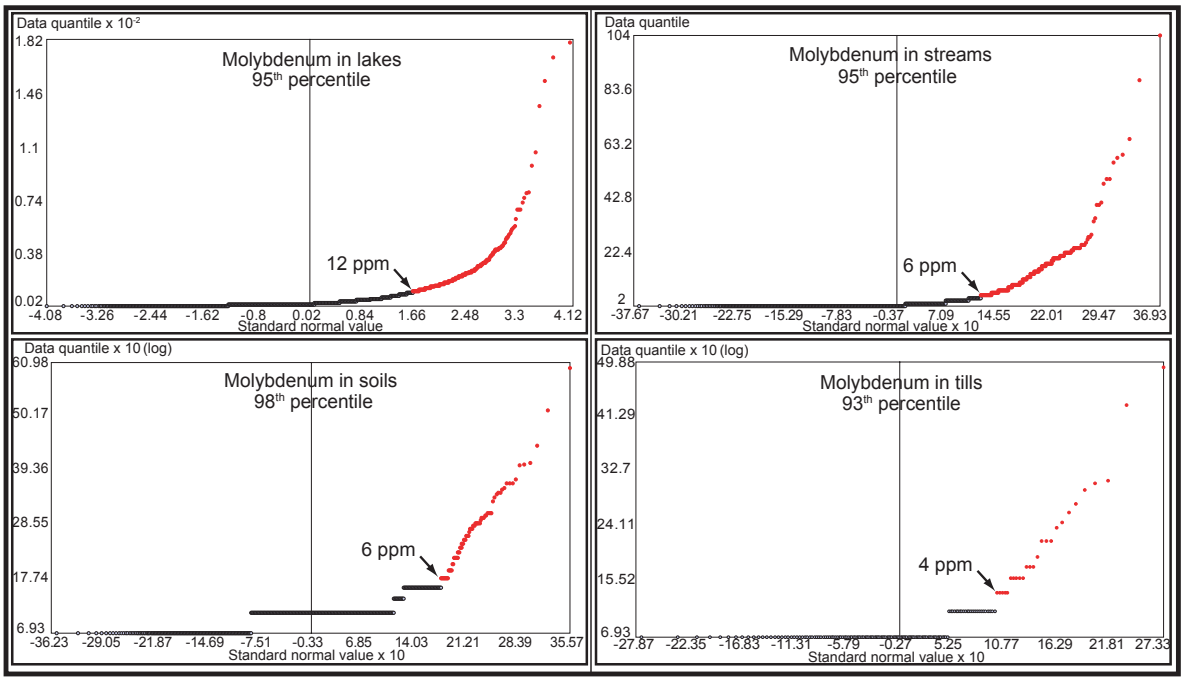

FIGURE 15 - Quantile-quantile plots used to define the anomalous threshold value for molybdenum in lake-bottom sediments, stream sediments, soils, and tills in the Baie-James region.

OVERALL FAVOURABILITY FOR PORPHYRY CU-AU ± MO DEPOSITS IN THE BAIE-JAMES REGION

Creation of a favourability map for porphyry-type Cu-Au ± Mo deposits in the Baie-James region

The final favourability map was created in two phases: 1) in each category (or sub-set), parameter maps generated using fuzzy values (Vfavor) calculated in Appendix 2 were combined using a FUZZYGAMMA operator (Appendix 3); and 2) the maps for all 5 categories were combined to create the final favourability map. The various factors for FUZZYGAMMA operators (in parentheses on the figure in Appendix 3) were calibrated relative to the predictivity of the combined parameters, taking into account as the main requirement the need to obtain, on the final map, a background value of about 0.5. This method helps prevent overweighing of parameters (a drawback often encountered when fuzzy logic is used as a combination method), while adhering to the principle of lack of

association, either favourable or unfavourable, in extensive parts of the region where the level of knowledge is low (areas in dark blue in Figure 21). The background value of the favourability map is 0.503 and the highest value recorded for all cells is 0.899.

Map of favourability associated with heat sources

The map showing the favourability associated with heat sources[1] is the result of the conversion, into fuzzy values, of contrast values for the different classes of the single parameter in this category (see Appendix 2 and 3). The highest fuzzy value in this map is 0.656 – a rather low value compared to maps in other categories and sub-sets (Figures 16a to 16h).

Map of favourability associated with lithological control

Figure 16a shows the various parts of the area where lithological control has the most influence in the selected ore deposit model. These areas correspond to locations where felsic or intermediate porphyry intrusions were reported near hematite or magnetite observations in the same rock types. The combination of these two parameter maps associated with lithological control was performed with a FUZZYGAMMA operator to which a factor of 0.80 was applied. A higher factor would have been contraindicated since these two parameters ranked in the lower third of the parameter ranking for predictivity (Appendix 2). The highest value on this map is 0.862.

The map shows a concentration of higher values around the La Grande 3 and Opinaca reservoirs (Figure 16a). Another favourable zone is visible southwest of Lac Tilly, while another cluster of scattered anomalies is visible around Lac Elmer and Opinaca Reservoir (33C). The area around Lac Troilus does not stand out in this part of the modelling due to the lack of *Géofiches* and compilation outcrop descriptions in this area, which severely limits the data response during processing.

Map of favourability associated with structural control

Anomalous areas on the map showing the favourability associated with structural control (Figure 16b) represent areas where a majority of the six parameters in this category overlap. These parameters, dominated by linear features or density zones, were combined using a FUZZYGAMMA operator to which a factor of 0.92 was applied (Appendix 3). The ranking, in the lower two thirds (except for one parameter) of the parameter ranking for predictivity, explains the choice of this relatively moderate factor. The highest value recorded on this map is 0.878.

Four zones largely stand out (Figure 16b): 1) the Lac Yasinski area, where the northeast tip of the Amisach Wat post-volcanic pluton (Goutier *et al.*, 1998) exhibits a large favourable zone; 2) the area south of Sakami, which extends toward Lac Guyer; 3) the shores of Opinaca Reservoir, south of which an E-W band extends for about 175 km between Lac Lichteneger and the western edge of the map; and 4) another E-W band about 170-km long, between Lac Le Gardeur and Lac Troilus, which corresponds to the Frotet-Evans belt.

Map of favourability associated with indicator metal analyses

The map showing the favourability associated with indicator metal analyses (Figure 16c) shows zones where a majority of anomalous values in Cu, Au, Mo, Ag, As, or W overlap. It was created with a FUZZYGAMMA operator to which a factor of 0.97 was applied. This high factor is justified by the fact that the six metallic parameters in this category rank in the top third of the parameter ranking for predictivity. The highest value recorded on this map is 0.988, which is the highest value for all intermediate maps in the combination process.

The highest values are concentrated (Figure 16c): 1) in rocks of the La Grande greenstone belt from Lac Yasinski to about 70 km east of Lac Guyer; 2) west of Lac Tilly; 3) between Lac Boyd and Lac Lichteneger, where high values form a scattered constellation with no apparent clustering; 4) in rocks of the Lower Eastmain greenstone belt, about 50 km northeast of Lac Marbois (NTS 33A), where major Cu-Mo ± Au deposits are known (among which the MacLeod Lake deposit); 5) in the vicinity of Lac Le Gardeur; 6) around Lac Troilus, where a Cu-Au mine is currently in operation; and 7) south of Lac Waconichi.

1 Since the map is nearly identical to that in Figure 9, it is not illustrated in Figure 16.

Map of favourability associated with alteration minerals

The map showing the favourability associated with alteration minerals (Figure 16d) shows zones where the majority of the five alteration facies under scrutiny overlap. It was obtained by combining parameters in this category (Appendix 3) using a FUZZYGAMMA operator to which a factor of 0.92 was applied. This relatively moderate factor may be explained by the fact that most of the parameters in this sub-set fall in the middle third of the parameter ranking for predictivity. The highest value recorded on this map is 0.932.

The distribution of high values in Figure 16d is very similar to that in Figure 16c, with the exception of the Opinaca-Lichteneger area, which seems to be less clearly defined in this case. Another zone located 50 km north of Lac La Salle (33H) also shows a few targets that appear to be better defined on this map relative to previous maps.

Map of favourability associated with NORMAT alteration indices

Figure 16e shows the map of favourability associated with NORMAT alteration indices. It is the result of the combination of favourability maps for the sericitization index (ISER) and the chloritization index (ICHLO) using a FUZZYGAMMA operator to which a factor of 0.95 was applied (Appendix 3). High values illustrated in the figure (maximum 0.954) correspond to zones where anomalous normative potassic alteration or chloritization compositions overlap. The two parameters rank in the middle third of the parameter ranking for predictivity.

The map shows the same clusters as the two previous maps, albeit with less clearly defined concentrations. Two notable exceptions are visible: strong concentrations in the Lac Elmer area (33C) and near Ile Bohier (33A).

Map of favourability associated with sulphides or oxides

The map showing the favourability associated with sulphides (Figure 16f) is the result of the combination of the six parameters in this category using a FUZZYGAMMA operator to which a factor of 0.95 was applied (Appendix 3). Except for chalcopyrite and bornite, both of which rank in the first third, all other minerals are less effective indicators, plotting in the middle or lower third of the parameter ranking for predictivity. The highest values on this map (maximum 0.881) correspond to zones where several sulphide (and/or magnetite) observations are reported.

The map in Figure 16f shows that the most favourable zones are located in the La Grande belt, the Lower and Middle Eastmain belt, and the Frotet-Evans belt. Zones northeast of Lac La Salle (33H) and Lac Marbois (33A) are also favourable. A linear zone to the west of Lac Evans (32K), also visible on the map in Figure 16c (metal indicators), is clearly defined. Visible in all previous maps, the Lac Tilly zone is conspicuously absent from this phase of processing. Finally, a small zone is visible about 40 km east of Nemiscau, along the *Route du Nord*. This zone, also visible in Figure 16c and 16d, is highlighted due to the overlapping presence of various sulphides (CP+MO+PY+PO) but is not associated with a known deposit.

Map of favourability associated with hydrothermal activity

The map showing the favourability associated with hydrothermal activity (Figure 16g) documents zones within the study area where hydrothermal activity played a major role within the scope of the selected ore deposit model. It was created by combining maps in figures 16c to 16f using a FUZZYGAMMA operator to which a factor of 0.82 was applied (Appendix 3). This low value for the modulating factor is due to: 1) the need to maintain the background value in the model at about 0.5; and 2) the four sub-sets composing this category have already been weighed individually in terms of their relative importance, it would thus be inappropriate to exaggerate the result of their combination by using a high factor. The maximum value recorded is 0.932.

The strongest zones are mainly located in the La Grande belt and the Frotet-Evans belt. In the former, favourable zones occur northeast of Lac Yasinski, west of Lac Sakami, and southeast of Robert-Bourassa Reservoir (33F) and in the Lac Guyer area (33G). In the latter, the main favourable zone occurs north of Lac Troilus (32J). A third significant zone is also visible, in the Lac Elmer area (33C).

Map of favourability associated with evidence in the secondary environment

Figure 16h shows zones where anomalous Cu, Au, or Mo grades in the secondary environment overlap most significantly. This map is the result of the combination of the three parameters in this category using a FUZZYGAMMA operator to which a factor of 0.80 was applied. The fact that these indicators rank in the lower third of the parameter ranking for predictivity explains the reasoning behind this low factor. The maximum value recorded is 0.764.

Figure 16h shows three significant zones in the area: 1) an E-W belt of about 70 km strike length, centred on Sakami (33F and 33G); 2) a N-S-trending zone of about 10 km located west of Lac Tilly; and 3) a NE-SW-trending zone of about 40 km strike length, centred on Lac Troilus. Two other discrete anomalies are visible near Opinaca Reservoir and west of Lac Waconichi.

Favourability map for porphyry-type Cu-Au ± Mo deposits

Figure 17 shows the favourability for porphyry-type Cu-Au ± Mo deposits in the Baie-James region. This map represents the end result of a combination process involving the integration of maps from the five broad categories in the model. The combination was performed using a FUZZYGAMMA operator to which a factor of 0.905 was applied, in order to reach the initial objective of having a background value around 0.5. The maximum value on this map is 0.899.

Determination of high-favourability zones and targets

Now that the final favourability map has been created, it is now possible: 1) to delineate, for the Baie-James region, high-favourability zones (HFZ) associated with porphyry-type Cu-Au ± Mo deposits that can be used to focus mineral exploration efforts; and 2) to determine and document more specifically a certain number of targets consisting of those parts of HFZ that were not staked at the time of the study.

Defining high-favourability zones involves establishing a minimum favourability threshold beyond which the favourability of a zone acquires a significant predictivity of the presence of porphyry-type mineralization. To define this threshold, overall favourability values associated with the 72 mines, deposits with tonnage estimates, worked deposits and showings in the Baie-James region were plotted on a normal probability diagram (Figure 18), which shows two distinct normal populations. The most important (red dots) includes 58 (80.5%) of the 72 documented porphyry deposits in the study area and lies above a minimum threshold value of 0.637. The 13 deposits that fall below the threshold form a second distinct population, that the favourability map cannot target effectively due to insufficient or contradictory data.

Using the minimum threshold value, it is possible to define, based on the final favourability map, a set of cells with values equal to or greater than 0.637 and to convert these groups of cells into polygons. These polygons constitute high-favourability zones (Figure 19).

The final list of targets was established using the distribution of active and pending titles as of November 1st, 2008. Parts of HFZ that were not staked at that time were selected to constitute 198 high-potential targets for porphyry Cu-Au ± Mo deposits. The latter are displayed on maps at various scales enclosed with this report and easily accessible in Appendix 4. A hyperlink attached to the label of each target provides direct access to an Access file with abundant relevant data for the target.

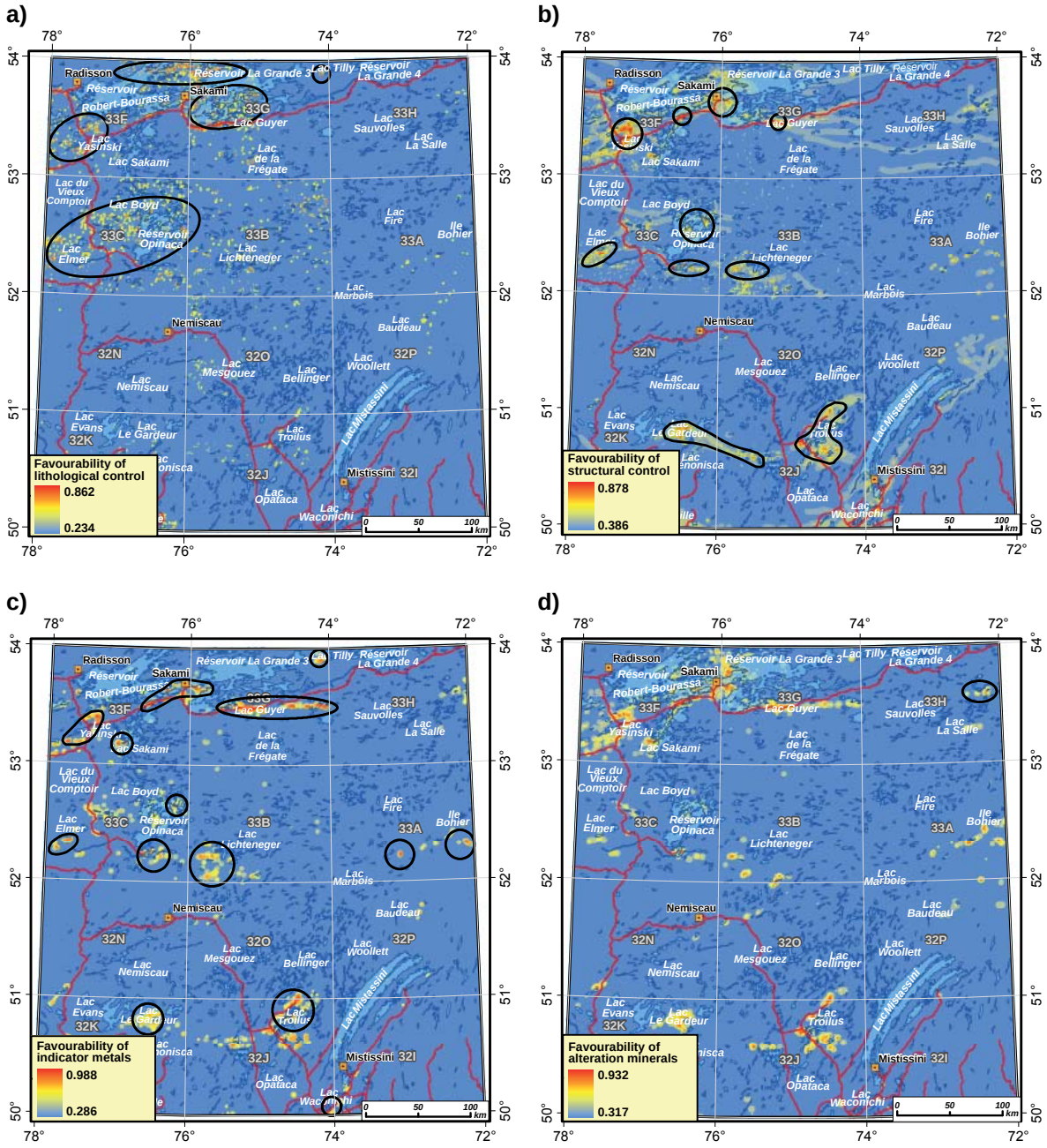

FIGURE 16 - a) favourability associated with lithological control; **b)** favourability associated with structural control; **c)** favourability associated with indicator metals; and **d)** favourability associated with alteration minerals.

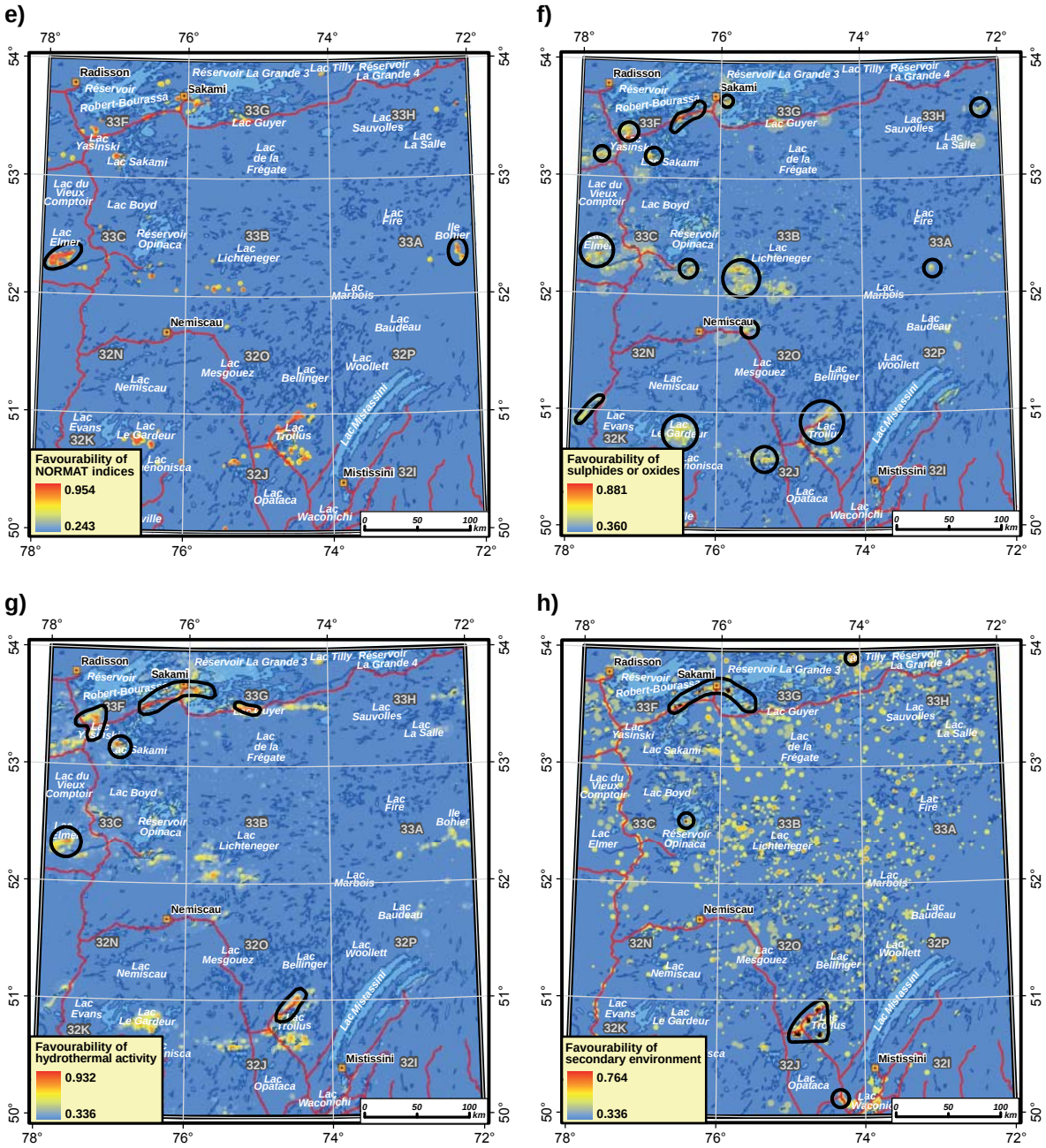

FIGURE 16 (continued) - e) favourability associated with NORMAT indices; **f)** favourability associated with sulphide or oxide occurrences; **g)** favourability associated with hydrothermal activity; and **h)** favourability associated with evidence in the secondary environment.

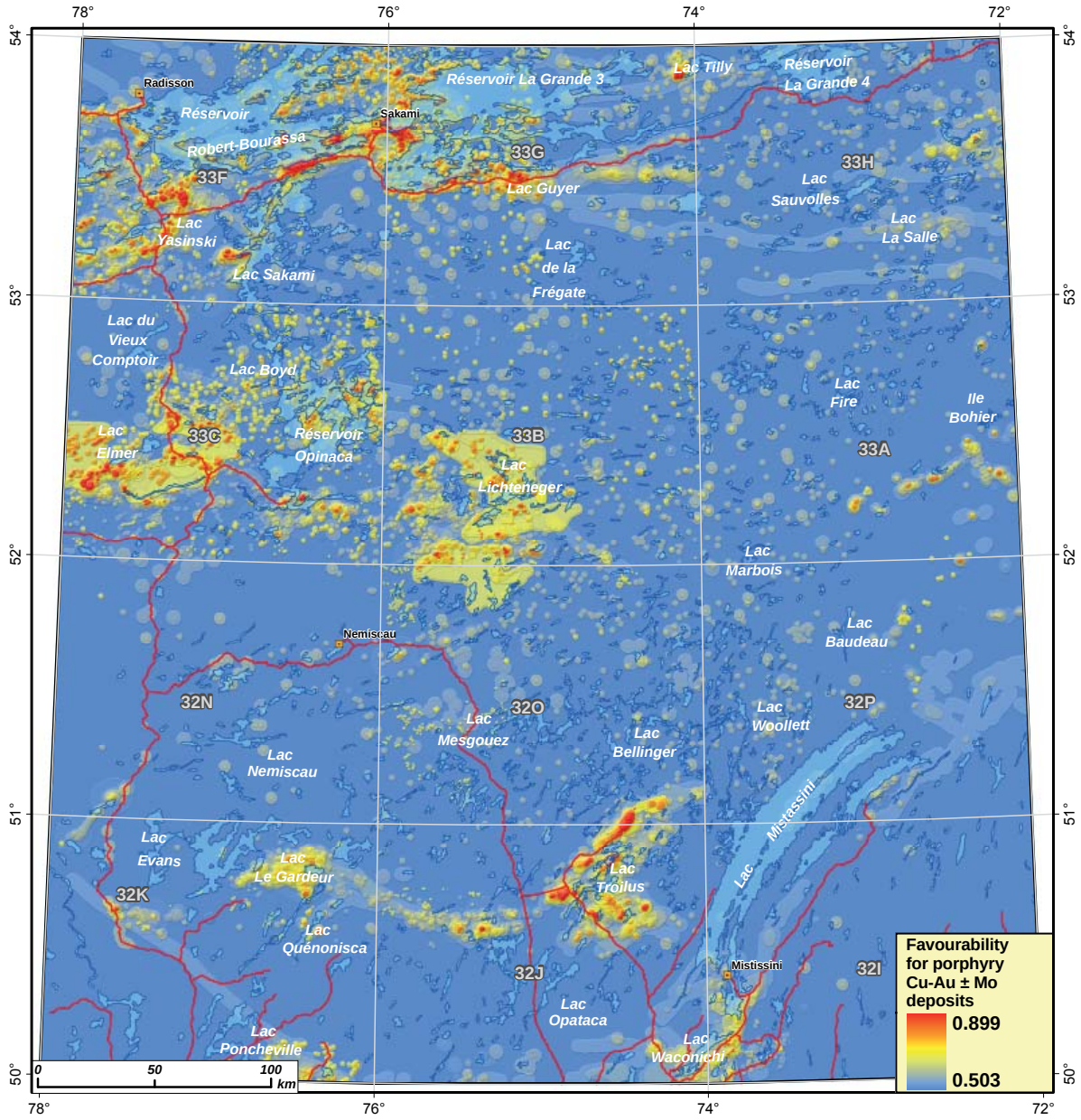

FIGURE 17 - Favourability for porphyry-type Cu-Au ± Mo deposits in the Baie-James region.

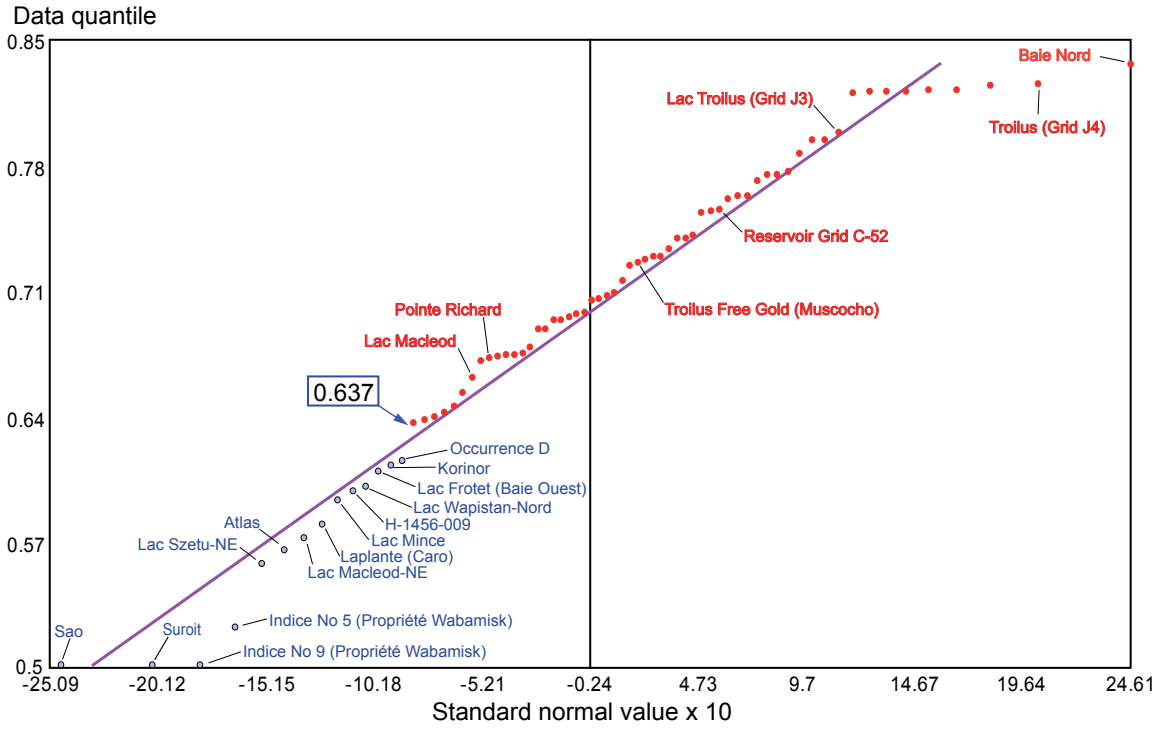

FIGURE 18 - Determination of the minimum high-favourability threshold using a normal probability plot. Values observed on the y axis correspond to the favourability value measured on the final favourability map for each of the 72 porphyry deposits. This type of diagram is used to distinguish different populations within a set. 80.5% of all porphyry deposits in the Baie-James region show a favourability value greater than 0.637 and form a homogeneous population that meets the model criteria, with measured favourability values following a Gaussian distribution. The most important deposits in this population are labelled in red. The 13 deposits in blue fall below the high-favourability threshold (0.637) and do not respond well to the model.

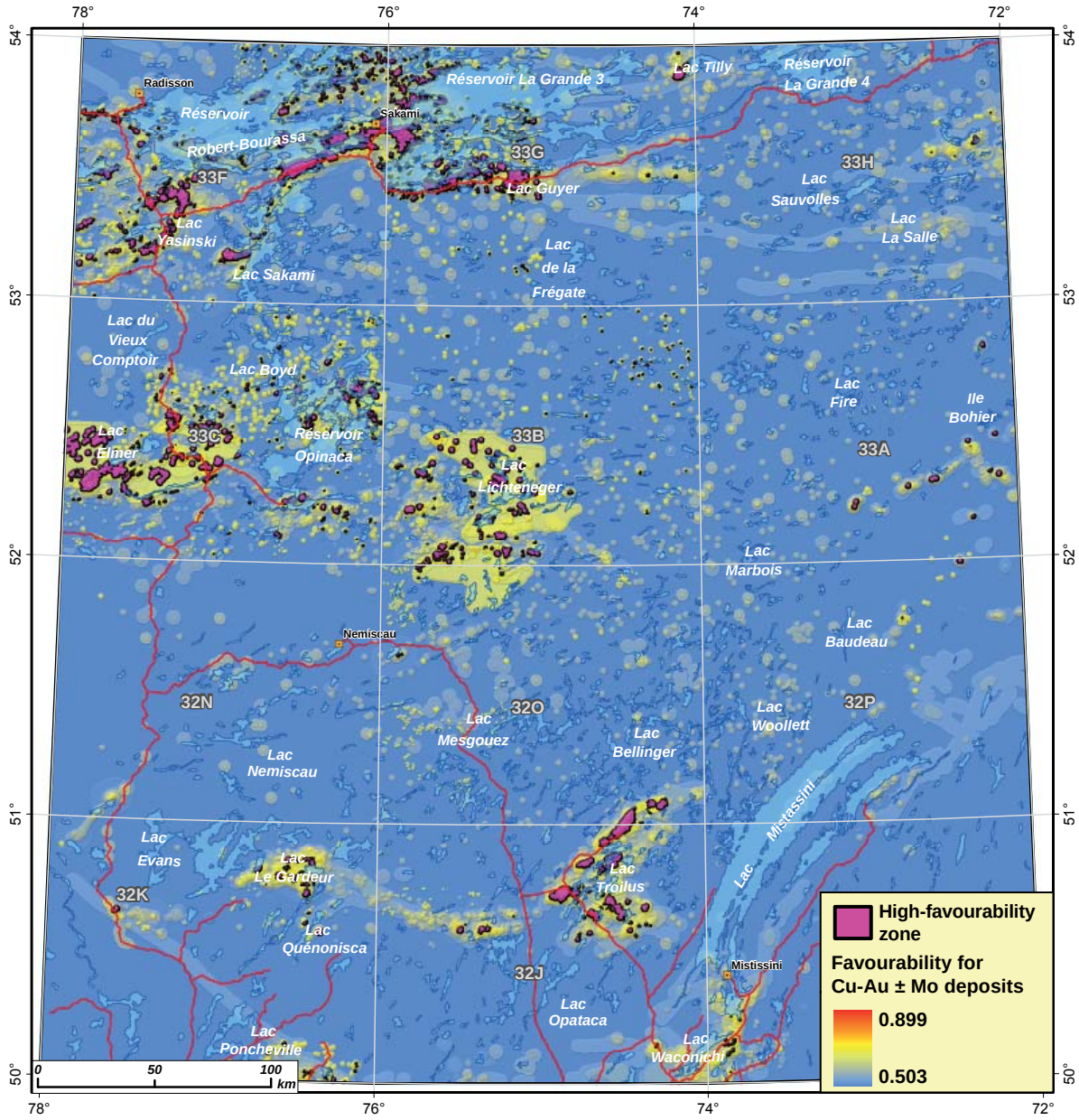

FIGURE 19 - Location of high-favourability zones (in purple) for porphyry-type deposits in the Baie-James region. For more details, see accompanying maps.

Validation of results

Figure 20a shows a diagram illustrating the predictivity of the favourability map for two sets of porphyry occurrences in the Baie-James region, namely: 1) a weighing set composed of 61 mines, deposits with a tonnage estimate, worked deposits, and showings, used to generate the favourability map; and 2) a control set of 11 deposits that were not used in processing but that can be used to validate the results. The graphs show the cumulative percentage of targeted deposits (on the y axis) versus the surface area covered (in cumulative percentage) by cells on the map sorted in decreasing order of favourability (on the x axis). The near-perfect overlap of the two curves shows that the favourability map has been validated by the control set and is thus reliable.

Figure 20b represents a close-up of the left part of the diagram in Figure 20a. This figure shows that 89.5% of deposits in the weighing set, and 93% of deposits in the control set are predicted by 5% of the surface area with the highest favourability rating. The predictivity of the favourability map is satisfactory, albeit lower than that obtained for orogenic gold deposits in the north part of the study area (Lamothe, 2008), where the same percentage of deposits was predicted in 1% of the surface area with the highest favourability. This difference is most likely due to the decision to use deposits classified as showings in both the weighing set and the control set. The much higher effectiveness of certain deposit types (particularly mines and deposits with tonnage estimates) to define the mineral favourability of an area has been demonstrated by Lamothe and Harris (2006) and by Harris and Sanborn-Barrie (2006). Deposit types such as mines, deposits with tonnage estimates, worked deposits, and showings are generally characterized by a respectively decreasing amount of spatial data, namely in terms of drill hole data and rock analyses. In particular, the greater volume of data associated with mines and deposits with tonnage estimates contributes to a robust definition of their geological attributes and therefore their eventual association with a parameter. Conversely, showings are commonly studied to a lesser extent and their immediate surroundings are generally poorly characterized, and this lower level of knowledge negatively impacts a certain number of parameters (lack of drill hole observations, limited sampling, deficient classification). Although useful – and even necessary in this case – the presence of these mineralized bodies in the modelling contributes to diluting the predictivity of most parameters.

The favourability map at 1/500,000 scale enclosed with this report was published on November 25, 2008. One of the HFZ defined through processing covers the Escale property (33H09) held by Sirios Resources. When the favourability map was published, Sirios Resources simultaneously issued a press release announcing the discovery of mineralized boulders with Au-Mo on the property. These boulders represent a new type of mineralization recognized on the Escale property, essentially explored until then for its potential for auriferous iron formations. The processing used for the porphyry ore deposit model appears to have correctly predicted this occurrence.

a) **b)**

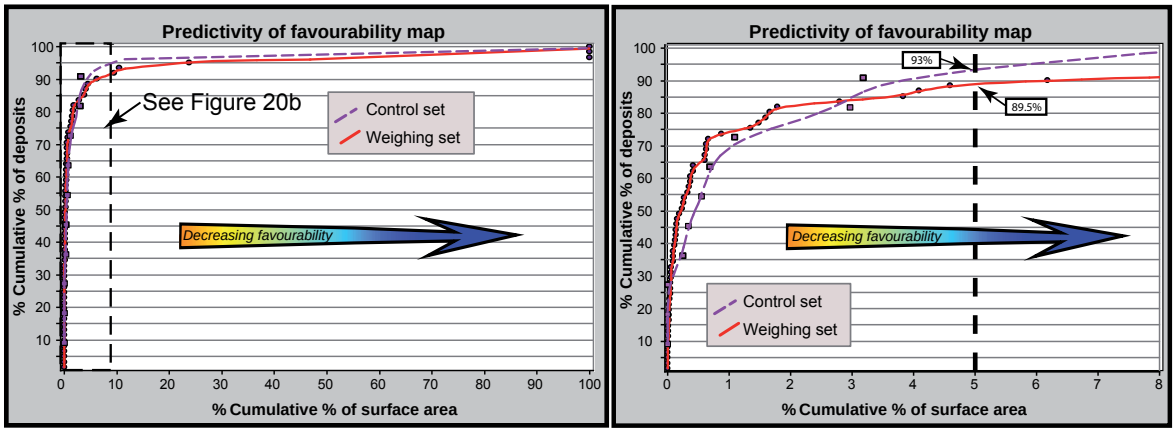

FIGURE 20 - a) Diagram illustrating the predictivity of the favourability map generated using "hybrid fuzzy logic". The diagram shows on the x axis the cumulative surface area (as a percentage) of cells sorted in decreasing order of favourability, and on the y axis, the cumulative percentage of deposits targeted by these cells.
b) Close-up of diagram 20a. About 89.5% of the 61 porphyry-type deposits used for processing (weighing set, in red) are located in the most favourable cells corresponding to 5% of the surface area on the map. Within the same favourable surface area, 93% of the 11 deposits in the control set (not used for processing, in violet) within the study area are targeted.

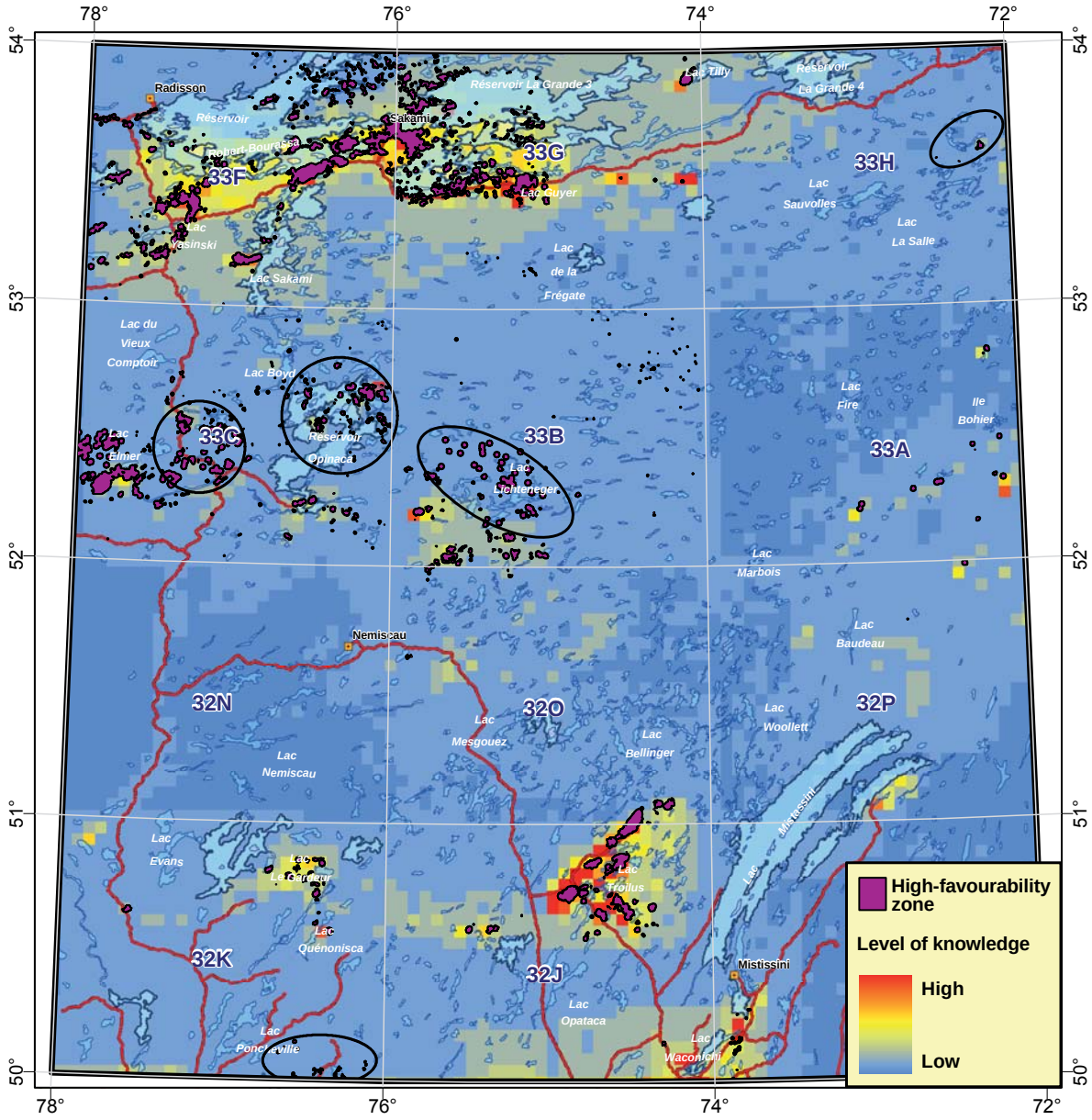

FIGURE 21 - Circled areas on this map are characterized by a strong concentration of HFZ despite their location in areas where the level of geological knowledge is lower. These areas are theoretically more favourable to the discovery of new deposits.

CONCLUSION

Integration of geodata using a "hybrid fuzzy logic" approach to processing has led to the creation of a reliable favourability map for the porphyry Cu-Au ± Mo ore deposit model. Its predictivity is acceptable, although lower than that achieved in previous potential assessment studies in the Abitibi and Baie-James regions. By establishing a minimum high-favourability threshold, the most prospective zones for new discoveries within the study area were delineated. These high-favourability zones (HFZ) should be the focus of further exploration work. This study also brings attention to 198 zones that remained unstaked as of November 1st, 2008, in order to signal the presence of new areas open to exploration.

Two conclusions can be drawn when looking at the distribution of HFZ on the map showing the level of knowledge in the same area (Figure 21): 1) the higher level of knowledge may explain the abundance of HFZ in the La Grande and Frotet-Evans belts; and 2) the level of knowledge cannot explain the presence of HFZ east of Lac Elmer and around Opinaca Reservoir (33C), northeast of Lac Lichteneger (33B), at the eastern edge of 33H, and south of Lac Poncheville (32K). In most of these 5 zones, exploration is relatively less advanced, and no porphyry deposits are known nearby that could explain this prospective setting. These zones are theoretically more favourable to the discovery of new deposits.

REFERENCES

AGTERBERG, F.P., 1989 – Systematic approach to dealing with uncertainty of geoscience information in mineral exploration. Proceedings 21st APCOM Symposium, Las Vegas, March 1989; Chapter 18, pages 165-178.

AGTERBERG, F.P. – BONHAM-CARTER, G.F. – WRIGHT, D.F., 1990 – Statistical pattern integration for mineral exploration. *In*: Computer Applications in Resource Estimation Prediction and Assessment for Metals and Petroleum (Gaal, G. and Merriam, D.F., editors). Pergamon Press, Oxford; pages 1-21.

AN, P. – MOON, W.M. – RENCZ, A.N., 1991 – Application of fuzzy theory for integration of geological, geophysical and remotely sensed data. Canadian Journal of Exploration Geophysics; Volume 27, pages 1-11.

AN, P. – MOON, W.M. – BONHAM-CARTER, G.F., 1992 – On a knowledge-based approach of integrating remote sensing, geophysical and geological information. Proceedings IGARSS'92; pages 34-38.

BOLENEUS, D.E. – RAINES, G.L. – CAUSEY, D. – BOOKSTROM, A.A. – FROST, T.P. – HYNDMAN, P.C., 2001 – Assessment method for epithermal gold deposits in northeast Washington State using weights-of-evidence GIS modelling. USGS; Open File report 01-501, 53 pages.

BONHAM-CARTER, G.F., 1994 – Geographic Information Systems for geoscientists: Modelling with GIS. Pergamon Press, Oxford; 398 pages.

BONHAM-CARTER, G.F. – AGTERBERG, F.P. – WRIGHT, D.F., 1988 – Integration of geological datasets for gold exploration in Nova Scotia. Photogrammetric Engineering and Remote Sensing; Volume 54, No.77, pages 1585-1592.

BONHAM-CARTER, G.F. – AGTERBERG, F.P. – WRIGHT, D.F., 1989 – Weights of evidence modelling: a new approach to mapping mineral potential. Statistical applications in the Earth Sciences; Geological Survey of Canada; Paper 89-9, pages 171-183.

BROWN, W. – GROVES, D.I. – GEDEON, T., 2003 – Use of fuzzy membership input layers to combine subjective geological knowledge and empirical data in a neural network method for mineral potential mapping. Natural Resources Research; Volume 12, No.3, pages 183-200.

BROWN, W.M. – GEDEON, T.D. – GROVES, D.I. – BARNES, R.G., 2000 – Artificial neural networks; a new method for mineral prospectivity mapping. Australian Journal of Earth Sciences; Volume 47, No.4, pages 757-770.

BURNHAM, C.W., 1979 – Magmas and hydrothermal fluids. In: Geochemistry of Hydrothermal Ore Deposits (Barnes, H.L. editor). John Wiley & Sons, New York, p. 71-136.

BUSHNELL, S.E., 1988 – Mineralization at Cananea, Sonora, Mexico, and the paragenesis and zoning of breccia pipes in quartzofeldspathic rock. Economic Geology, Volume 83, pages 1760-1781.

CALVERT, A.J. – SAWYER, E.W. – DAVIS, W.J. – LUDDEN, J.N., 1995 – Archean subduction inferred from seismic images of a mantle suture in the Superior Province. Nature, Volume 375, pages 670-674.

CARD, K.D. – CIESIELSKI A., 1986 – Subdivisions for the Superior Province of the Canadian Shield. Geoscience Canada; Volume 13, pages 5-13.

CARRANZA, E.J.M. – HALE, M., 2000 – Geologically Constrained Probabilistic Mapping of Gold Potential, Baguio District, Philippines. Natural Resources Research; Volume 9, No. 3, pages 237-253.

CARRANZA, E.J.M. – HALE, M., 2002 – Where are Porphyry Copper Deposits Spatially localized? A case study in Benguet Province, Philippines. Natural Resources Research; Volume 11, No. 1, pages 45-59.

CHENG, Q. – AGTERBERG, F.P., 1999 – Fuzzy weights of evidence and its application in mineral potential mapping. Natural Resources Research; Volume 8, No. 1, pages 27-35.

CHUNG, C.F. – AGTERBERG, F.P., 1980 – Regression models for estimating mineral resources from geological map data. Mathematical Geology; Volume 12, No.5, pages 473-488.

CHUNG, C.F. – MOON, W.M., 1991 – Combination rules of spatial geoscience data for mineral exploration. Geoinformatics; Volume 2, pages 159-169.

D'ERCOLE, C. – GROVES, D.I. – KNOX-ROBINSON, C.M., 2000 – Using fuzzy logic in a Geographic Information System environment to enhance conceptually based prospectivity analysis of Mississippi Valley-type mineralization. Australian Journal of Earth Sciences; Volume 47, pages 913-927.

DE ARAUJO, C.C. – MACEDO, A.B., 2002 – Multicriteria geologic data analysis for mineral favourability mapping: Application to a metal sulphide mineralized area, Ribeira Valley Metallogenic Province, Brazil. Natural Resources Research; Volume 11, No. 1, pages 29-43.

DION, C. – LAMOTHE, D., 2002 – Évaluation du potentiel en minéralisations de sulfures massifs volcanogènes de la région de Chibougamau (32G) - Intégration de géodonnées par la technologie d'analyse spatiale. Ministère des Ressources naturelles; EP 2002-04, 1 CD-ROM.

FRASER, R.J., 1993 – The Lac Troilus gold-copper deposit, Northwestern Quebec: a possible Archean porphyry system. Economic Geology; Volume 88, pages 1685-1699.

GAÁL, G. – ISOHANNI, M., 1979 – Characteristics of igneous intrusions and various wall rocks in some Precambrian porphyry copper-molybdenum deposits in Pohjinamaa, Finland. Economic Geology; Volume 74, pages 1198-1210.

GAUTHIER, M. – LAROQUE, M. – CHARTRAND, F., 1997 – Cadre géologique, style et répartition des minéralisations métalliques de la Grande Rivière, territoire de la Baie-James. Ministère des Ressources naturelles, MB 97-30, 69 pages.

GAUTHIER, M. – LAROQUE, M., 1998 – Cadre géologique, style et répartition des minéralisations métalliques de la Basse et de la Moyenne Eastmain, territoire de la Baie-James. Ministère des Ressources naturelles; MB 98-10, 86 pages.

GAUTHIER, M. – TRÉPANIER, S. – GARDOLL, S., 2007 – Metamorphic gradient: A regional-scale area selection criterion for gold in the Northeastern Superior province, Eastern Canadian Shield. SEG Newsletter; Volume 69, pages 9-15.

GILMOUR, P., 1977 – Mineralized intrusive breccias as guides to concealed porphyry copper systems. Economic Geology, Volume 72, pages 290-298.

GOUTIER, J. – DION, C. – OUELLET, M.C. – DAVIS, D.W. – DAVID, J. – PARENT, M., 2002 – Géologie de la région du lac Guyer (33G/05, 33G/06 et 33G/11). Ministère des Ressources naturelles, de la Faune et des Parcs; RG 2001-15, 53 pages.

GOUTIER, J. – DION, C. – OUELLET, M.C. – MERCIER-LANGEVIN, P. – DAVIS, D.W., 2001 – Géologie de la colline Masson (33F/09), de la passe Awapakamich (33F/10), de la baie Carbillet (33F/15) et de la passe Pikwahipanan (33F/16). Ministère des Ressources naturelles; RG 2000-10, 67 pages.

GOUTIER, J. – DOUCET, P. – BEAUSOLEIL, C. – DION, C. – DAVID, J. – PARENT, M. – DION, D.-J., 1998 – Géologie de la région du lac Kowskatehkakmow (SNRC 33F/06). Ministère des Ressources naturelles; RG 98-16, 48 pages.

GROVES, D.I. – GOLDFARB, R.J. – KNOX-ROBINSON, C.M. – OJALA, V.J. – GARDOLL, S.J. – YUN G. Y. – HOLYLAND P.W., 2000 – Late-kinematic timing of orogenic gold deposits and significance for computer based exploration techniques with emphasis on the Yilgarn Block, Western Australia. Ore Geology Reviews; Volume 17, pages 1-38.

HAGEMANN, S.G. – CASSIDY, K.F., 2000 – Archean orogenic lode gold deposits. *In*: Gold in 2000 (Hagemann, S.G. and Brown, P.E., editors). Reviews in Economic Geology; Volume 13, pages 9-68.

HARRIS, J.R., 1989 – Data Integration for gold exploration in eastern Nova Scotia using a GIS. *In*: Proceedings of Remote Sensing for Exploration Geology, Calgary, Alberta. Published by Environmental Research Institute of Michigan; pages 233-249.

HARRIS, D.A. – PAN, R., 1999 – Mineral favourability mapping: a comparison of artificial networks, logistic regression and discriminant analysis. Natural Resources Research; Volume 8, No.2, pages 93-109.

HARRIS, J.R. – SANBORN-BARRIE, M. – PANAGAPKO, D.A. – SKULSKI, T. – PARKER, J.R., 2006 – Gold prospectivity maps of the Red Lake greenstone belt: Application of GIS technology. Canadian Journal of Earth Sciences; Volume 43, pages 865-893.

HARRIS, J.R. – SANBORN-BARRIE, M., 2006 – Mineral potential mapping : Examples from the Red Lake greenstone belt, northwest Ontario. *In*: GIS for the Earth Sciences (Harris, J.R., editor). Geological Association of Canada; Special Paper 44, pages 1-22.

HARRIS, J.R. – WILKINSON, L. – BROOME, J., 1995 – Mineral exploration using GIS-based favourability analysis, Swayze Greenstone Belt, Northern Ontario. *In*: Proceedings of the Canadian Geomatics Conference (CD-ROM), National Defence Canada.

HARRIS, J.R. – WILKINSON, L. – GRUNSKY, E., 2000 – Effective use and interpretation of lithogeochemical data in regional mineral exploration programs: Application of Geographic Information System (GIS) technology. Ore Geology Reviews; Volume 16, pages 107-143.

HARRIS, J.R. – WILKINSON, L. – GRUNSKY, G. – HEATHER, K., AYER, J., 1999 – Techniques for analysis and visualization of lithogeochemical data with applications to the Swayze greenstone belt, Ontario. Journal of Geochemical Exploration; Volume 67, No.1-3, pages 301-334.

HARRIS, J.R. – WILKINSON, L. – HEATHER, K. – FUMERTON, S. – BERNIER, M.A. – AYER, J. – DAHN, R., 2001 – Application of GIS processing techniques for producing mineral prospectivity maps – A case study: Mesothermal Au in the Swayze greenstone belt, Ontario, Canada. Natural Resources Research; Volume 10, No.2, pages 91-124.

HOCQ, M., 1994 – La Province du Supérieur. *In*: Géologie du Québec. Ministère des Ressources naturelles; MM 94-01, pages 7-20.

HOLLISTER, V.F., 1985 – Models of precious metal epithermal deposits. In: Discoveries of epithermal precious metals deposits (Hollister, V.F. editor). Society of Mining Engineers, New York; 169 pages.

JENKS, G.F., 1967 – The Data Model Concept in Statistical Mapping. International Yearbook of Cartography; Volume 7, pages 186-190.

KIRKHAM, R.V. – SINCLAIR, W.D., 1996 – Porphyry copper, gold, molybdenum, tungsten, tin, silver. In: Geology of Canadian Mineral Deposit Types (Eckstrand, O.R., Sinclair, W.D. and Thorpe, R.I., editors). Geological Survey of Canada; Geology of Canada, No. 8, pages 421-446.

KNOX-ROBINSON, C.M., 2000 – Vectorial fuzzy logic: a novel technique for enhanced mineral prospectivity mapping, with reference to the orogenic gold mineralization potential of the Kalgoorlie Terrane, Western Australia. Australian Journal of Earth Sciences; Volume 57, No. 5, pages 929-942.

LABBÉ, J.-Y., 2002 – Évaluation du potentiel de découverte de kimberlites de la région du Grand-Nord du Québec - Intégration de géodonnées par la technologie d'analyse spatiale. Ministère des Ressources naturelles; EP 2002-05, 1 CD-ROM.

LABBÉ, J.-Y. – PILOTE, P. – LAMOTHE, D., 2006 – Assessment of the potential for porphyry Cu-Au-Mo deposits in the Abitibi. Ministère des Ressources naturelles et de la Faune; EP 2007-01, 1 CD-ROM.

LAMOTHE, D., 2008 – Assessment of the potential for orogenic gold deposits in the Baie-James region. Ministère des Ressources naturelles et de la Faune; EP 2008-02, 1 CD-ROM.

LAMOTHE, D. – BEAUMIER, M., 2001 – Évaluation du potentiel régional en minéralisations de type Olympic Dam-Kiruna dans la région du lac Manitou (SNRC 22I). Ministère des Ressources naturelles; EP 2001-01, 1 CD-ROM.

LAMOTHE, D. – BEAUMIER, M., 2002 – Évaluation du potentiel régional en minéralisations de type Olympic Dam-Kiruna dans la région du lac Fournier (SNRC 22P). Ministère des Ressources naturelles; EP 2002-01, 1 CD-ROM.

LAMOTHE, D. – HARRIS, J.R, 2006 – Assessment of the potential for orogenic gold deposits in the Abitibi. Ministère des Ressources naturelles et de la Faune; EP 2006-02, 1 CD-ROM.

LAMOTHE, D. – HARRIS, J.R. – LABBÉ, J.-Y. – DOUCET, P. – HOULE, P. – MOORHEAD, J., 2005 – Assessment of the potential for volcanogenic massive sulphide (VMS) deposits in Abitibi. Ministère des Ressources naturelles, de la Faune et des Parcs; EP 2005-02, 1 CD-ROM.

LAROUCHE, J., 2005 – Caractérisation de la minéralisation de la fosse J4 à la mine Troilus, Chibougamau. Université du Québec à Chicoutimi, Master's Thesis; 165 pages.

MOUKHSIL, A. – LEGAULT, M. – BOILY, M. – DOYON, J. – SAWYER, E. – DAVIS, D.W., 2003 – Geological and metallogenic synthesis of the Middle and Lower Eastmain greenstone belt (James Bay). Ministère des Ressources naturelles, de la Faune et des Parcs; ET 2007-01, 58 pages.

PAGANELLI, F. – RICHARDS, J.P. – GRUNSKY, E.C., 2002 – Integration of Structural, Gravity and Magnetic Data Using the Weights of Evidence Method as a tool for Kimberlite Exploration in the Buffalo Head Hills, Northern Central Alberta, Canada. Natural Resources Research; Volume 11, No. 3, pages 219-236.

PERRY, V.D., 1961 – The significance of mineralized breccia pipes. Mining Engineering, Volume 13, pages 367-376.

PICHÉ, M. – JÉBRAK, M., 2004 – Normative minerals and alteration indices developed for mineral exploration. Journal of Geochemical Exploration; Volume 82, pages 59-77.

PILOTE, P. – DION, C. – JOANISSE, A. – DAVID, J. – MACHADO, N. – KIRKHAM, R. – ROBERT, F., 1997 – Géochronologie des minéralisations d'affiliation magmatique de l'Abitibi, secteurs de Chibougamau et de Troilus-Frotet : Implications géotectoniques. *In*: Vers de nouvelles découvertes. Séminaire d'information sur la recherche géologique. Ministère des Ressources naturelles; Program with Abstracts, page 47.

PILOTE, P. – ROBERT, F. – KIRKHAM, R.V. – DAIGNEAULT, R. – SINCLAIR, W.D., 1998 – Porphyry-type mineralization in the Doré Lake Complex: Clark Lake and Merrill Island areas. *In*: Geology and Metallogeny of the Chapais-Chibougamau Mining District (Pilote, P., editor). Ministère des Ressources naturelles, Québec; DV 98-04, page 61-78.

PORWAL, A. – CARRANZA E.J.M. – HALE, M., 2003a – Artificial neural networks for mineral-potential mapping: A case study from the Aravalli Province, western India. Natural Resources Research; Volume 12, No. 3, pages 155-171.

PORWAL, A. – CARRANZA E.J.M. – HALE, M., 2003b – Knowledge-driven and data-driven fuzzy models for predictive mineral potential mapping. Natural Resources Research; Volume 12, No. 1, pages 1-25.

PORWAL, A. – HALE, M., 2000 – GIS-based weights-of-evidence analysis of multiclass spatial data for predictive mineral map ping: a case study from Aravalli province, western India: Proc. XIV Intern. Con. Applied Geologic Remote Sensing, (Las Vegas, Nevada); pages 377-384.

RAINES, G.L., 1999 – Evaluation of Weights of Evidence to predict epithermal gold deposits in the Great Basin of the western United States. Natural Resources Research; Volume 8, No.4, pages 257-276.

REDDY, R.K.T. – AGTERBERG, F.P. – BONHAM-CARTER, G.F., 1991 – Application of GIS-based logistic models to base-metal potential mapping in Snow Lake area, Manitoba. *In*: Proceedings Canadian Conference on GIS, Ottawa, Canada, March 18-22, 1991; pages 607-618.

RENCZ, A.N. – HARRIS, J.R. – WATSON, G.P. – MURPHY, B., 1994 – Data Integration for Mineral Exploration in the Antigonish Highlands, Nova Scotia. Canadian Journal of Remote Sensing; Volume 20, No.3, pages 258-267.

ROGGE, D.M. – HALDEN, N.M. – BEAUMONT-SMITH, C., 2006 – Application of Data Integration for Shear-Hosted Au Potential Modelling Linn Lake Greenstone Belt, Northwestern Manitoba, Canada. *In*: GIS for the Earth Sciences (Harris, J.R., editor). Geological Association of Canada; Special Paper 44, pages 191-210.

SAWYER, E.W. – BENN, K., 1993 – Structure of high-grade Opatica Belt and adjacent low-grade Abitibi Subprovince, Canada: an Archean mountain front. Journal of Structural Geology, Volume 15, pages 1443-1458.

SEEDORF, E. – DILLES, J.H. – PROFFET, J.M. – EINAUDI, M.T. – ZURCHER, L. – STAVAST, W.J.A. – JOHNSON, D.A. – BARTON, M.D., 2005 – Porphyry deposits: Characteristics and Origin of Hypogene Features. Economic Geology; 100th Anniversary Volume; pages 251-298.

SILLITOE, R.H.., 1985 – Ore-related breccias in volcanoplutonic arcs. Economic Geology; Volume 80, pages 1467-1514.

SILLITOE, R.H., 1989 – Gold deposits in Western Pacific islands arcs: the magmatic connection. *In*: The geology of gold deposits: the perspectives in 1988 (Keays, R.R., Ramsay,, W.R.H., and Groves, D.I., editors). Economic Geology Monograph 6; pages 274-291.

SILLITOE, R.H., 1993 – Gold–rich porphyry copper deposits: geological model and exploration implications. *In*: Mineral Deposit Modeling (Kirkham, R.V., Sinclair, W.D., Thorpe, R.I. and Duke, J.M., editors). Geological Association of Canada; Special Paper 40, pages 465–478.

SINGER, D.A. – KOUDA, R., 1996 – Application of feedforward neural network in search for Kuroko deposits in the Hokuroku district, Japan. Mathematical Geology; Volume 28, No.3, pages 1017-1023.

SINGER, D.A. – KOUDA, R., 1997a – Use of a neural network to integrate geoscience information in the classification of mineral deposits and occurrences. *In*: Proceedings of Exploration 97: 4th Decennial International Conference on Mineral Exploration (Gubins, A.G., editor). Pages 127-134.

SINGER, D.A. – KOUDA, R., 1997b – Classification of mineral deposits into types using mineralogy with a probabilistic neural network. Nonrenewable Resources; Volume 6, pages 27-32.

SINGER, D.A. – KOUDA, R., 1999 – A comparison of the weights-of-evidence method and probabilistic neural networks. Natural Resources Research; Volume 8, No. 4, pages 287-298.

SPIEGELHALTER, D.J., 1986 – Uncertainty in expert systems. *In*: Artificial Intelligence and Statistics (Gale, W.A., editor). Addison-Wesley, Reading, Massachusetts; pages 17-25.

TANGESTANI, M.H. – MOORE, F., 2003 – Mapping porphyry copper potential with a fuzzy model, northern Shar-e-Babak, Iran. Australian Journal of Earth Sciences, Volume 50, pages 311-317.

THÉRIAULT, R., 2002 – Geological map of Québec – Edition 2002. Ministère des Ressources naturelles et de la Faune, DV 2002-07, 8 pages.

THURSTON, P.C., 1991 – Archean Geology of Ontario: Introduction. *In*: Geology of Ontario. Ontario Geological Survey; Special Volume 4, part 1, pages 73-78.

TITLEY, S.R., 1993 – Characteristics of porphyry copper occurrence in the American Southwest. *In*: Mineral Deposit Modeling (Kirkham, R.V., Sinclair, W.D., Thorpe, R.I. and Duke, J.M., editors). Geological Association of Canada; Special Paper 40, pages 433–464.

TURNER, D.D., 1997 – Predictive GIS Model for Sediment-Hosted Gold Deposits, North-Central Nevada, U.S.A. *In*: Proceedings of Exploration 97 : Fourth Decennial International Conference on Mineral Exploration (Gubins, A.G., editor). Pages 115-126.

VILA, T. – SILLITOE, R.H., 1991 – Gold–rich porphyry systems in the Maricunga gold–silver belt, northern Chile. Economic Geology; Volume 86, pages 1238–1260.

WILKINSON, L. – HARRIS, J.R. – KEATING, P. – KJARSGAARD, B., 2006 – GIS spatial analysis tools to assist in the search for kimberlite: Weights of evidence applied to the Lac de Gras region. *In*: GIS for the Earth Sciences (Harris, J.R., editor). Geological Association of Canada; Special Paper 44, pages 211-228.

WILLIAMS, W.C. – MEISSL, E. – MADRID, J.- DE MACHUCA, B.C., 1999 – The San Jorge porphyry copper deposit, Mendoza, Argentina: a combination of orthomagmatic and hydrothermal mineralization. Ore Geology Reviews; Volume 14, No 3, pages 185-201.

WILLIAMS-JONES, A.E. – HEINRICH, C.A., 2005 – Vapor Transport of Metals and the Formation of Magmatic-Hydrothermal Ore Deposits. *In*: 100th Anniversary Special Paper. Economic Geology; Volume 100, No. 7, pages 1287-1312.

WRIGHT, D.F., 1996 – Evaluating volcanic hosted massive sulphide favourability using GIS-based spatial data integration models, Snow Lake area, Manitoba. Unpublished Ph.D. thesis, University of Ottawa; 338 pages.

WRIGHT, D.F. – BONHAM-CARTER, G.F., 1996 – VHMS Favourability Mapping with GIS-Based Integration Models, Chisel Lake-Anderson Lake Area. *In*: EXTECH I: A Multidisciplinary Approach to Massive Sulphide Research in the Rusty Lake- Snow Lake Greenstone Belts, Manitoba (Bonham-Carter, G.F., Galley, A.G., Hall, G.E.M., editors). Geological Survey of Canada; Bulletin 426, pages 339-376 and 387-401.

APPENDIX 1

Characteristics of deposits used to calculate weight factors and to validate the potential map for porphyry Cu-Au ± Mo deposits.

#	NTS	NAME	STATUS	ZONE	EASTING	NORTHING	TYPE	Vfavor(m)
1	33H15	Suroit	Showing	18	637380	5978081	Copper-rich veins	0.502
2	33G16	Silly Cat	Worked deposit	18	558768	5974321	Porphyry Cu-Au-Mo dep.	0.694
3	33G16	Brèche Ozzy	Worked deposit	18	559328	5973131	Porphyry Cu-Au-Mo dep.	0.706
4	33G16	Extension NE	Showing	18	560653	5972877	Porphyry Cu-Au-Mo dep.	0.724
5	33G16	Ricky	Showing	18	560094	5972432	Porphyry Cu-Au-Mo dep.	0.762
6	33G16	Firecracker	Worked deposit	18	557959	5972031	Porphyry Cu-Au-Mo dep.	0.794
7	33G16	Brèche Alix	Worked deposit	18	560428	5972031	Porphyry Cu-Au-Mo dep.	0.771
8	33G16	Brèche Yogi	Worked deposit	18	559628	5971931	Porphyry Cu-Au-Mo dep.	0.755
9	33G16	Brèche Boubou	Worked deposit	18	559978	5971901	Porphyry Cu-Au-Mo dep.	0.763
10	33G16	Brèche Ouest	Showing	18	557628	5971731	Porphyry Cu-Au-Mo dep.	0.754
11	33G16	Blue Fox-Nord	Showing	18	558228	5971431	Porphyry Cu-Au-Mo dep.	0.794
12	33G16	Blue Fox-Sud	Showing	18	558350	5971100	Porphyry Cu-Au-Mo dep.	0.775
13	33G16	Yo	Worked deposit	18	557978	5970901	Porphyry Cu-Au-Mo dep.	0.775
14	33F09	Digue	Showing	18	433351	5951941	Copper-rich veins	0.734
15	33F09	Orage	Worked deposit	18	419311	5949437	Copper-rich veins	0.640
16	33G12	Baie Nord	Showing	18	438081	5947121	Copper-rich veins	0.836
17	33F09	Chain-Lake	Showing	18	432188	5947117	Copper-rich veins	0.637
18	33G12	Tyrone 4	Showing	18	439275	5946780	Copper-rich veins	0.821
19	33G12	Tyrone 5	Worked deposit	18	438809	5946602	Copper-rich veins	0.822
20	33G12	Tyrone 2	Worked deposit	18	439831	5946056	Copper-rich veins	0.821
21	33G12	Tyrone 1	Worked deposit	18	439824	5945939	Copper-rich veins	0.821
22	33F09	Sommet 4	Worked deposit	18	412726	5943668	Copper-rich veins	0.822
23	33F09	Jameson	Showing	18	412381	5943592	Copper-rich veins	0.821
24	33F09	Marjolaine	Worked deposit	18	412563	5943583	Copper-rich veins	0.825
25	33G12	Tournesol	Showing	18	447348	5942977	Copper-rich veins	0.689
26	33F09	Aéroport-B	Showing	18	428372	5941131	Copper-rich veins	0.694
27	33F09	Veine Sawyer	Worked deposit	18	410887	5935819	Copper-rich veins	0.763
28	33F10	Karine	Showing	18	400183	5934633	Copper-rich veins	0.698
29	33F05	Lac Szetu-NE	Worked deposit	18	320209	5931197	Copper-rich veins	0.558
30	33H05	Sao	Showing	18	575160	5908453	Porphyry Cu-Au-Mo dep.	0.502
31	33F04	Korinor-Taylor	Showing	18	330112	5896174	Copper-rich veins	0.730
32	33F04	Korinor	Showing	18	327674	5895250	Copper-rich veins	0.613
33	33F04	Lac Wapistan-Nord	Showing	18	327583	5894341	Copper-rich veins	0.601
34	33C09	Lac Ell	Worked deposit	18	423622	5835594	Porphyry copper	0.741
35	33A08	Lac Michel	Worked deposit	18	695980	5800705	Dep. assoc. with porphyry intr.	0.698
36	33C05	Indice 2308-23 (SDBJ)	Worked deposit	18	308882	5796410	Porphyry copper	0.674
37	33C05	Indice 2308-18 (SDBJ)	Worked deposit	18	308541	5795789	Porphyry copper	0.675
38	33C05	Lac Kali	Worked deposit	18	307241	5794720	Dep. assoc. with porphyry intr.	0.777
39	33C05	2308-11(SDBJ)	Worked deposit	18	307470	5794120	Porphyry copper	0.739
40	33C05	2308-16 (SDBJ)	Worked deposit	18	307900	5794120	Porphyry copper	0.679
41	33C05	2308-13 (SDBJ)	Worked deposit	18	307624	5793977	Porphyry copper	0.739
42	33C05	Clouston	Showing	18	322171	5792245	Porphyry Cu-Au-Mo dep.	0.728
43	33C07	Indice No 5 (Propriété Wabamisk)	Showing	18	377777	5791255	Copper-rich veins	0.523
44	33C08	Reservoir Grid C-52	Dep. with tonnage est.	18	398276	5790584	Porphyry Cu-Au-Mo dep.	0.756
45	33C02	Indice No 9 (Propriété Wabamisk)	Showing	18	381602	5790205	Copper-rich veins	0.502
46	33A02	Lac Macleod-NE	Worked deposit	18	637329	5789480	Porphyry Cu-Au-Mo dep.	0.572
47	33C02	Zone Cyr	Worked deposit	18	391048	5789210	Dep. assoc. with porphyry intr.	0.671
48	33C02	Bear Island (Wabamisk)	Worked deposit	18	392788	5789050	Copper-rich mantos	0.710
49	33C02	Wab-88-04/06	Worked deposit	18	390394	5788619	Dep. assoc. with porphyry intr.	0.705
50	33A03	Lac Macleod	Dep. with tonnage est.	18	634454	5788250	Porphyry Cu-Au-Mo dep.	0.662
51	33A03	Pointe Rocky	Worked deposit	18	633804	5787280	Porphyry Cu-Au-Mo dep.	0.646
52	33A03	Pointe Richard	Dep. with tonnage est.	18	634254	5786305	Porphyry Cu-Au-Mo dep.	0.673
53	33B04	Lac Mince	Worked deposit	18	455190	5785748	Copper-rich veins	0.594
54	33B04	Rosemary NE	Worked deposit	18	442791	5785087	Porphyry Cu-Au-Mo dep.	0.675
55	33B04	Rosemary (Indices à Robert)	Worked deposit	18	441870	5784689	Porphyry Cu-Au-Mo dep.	0.674
56	33B03	Addison	Showing	18	472040	5780995	Copper-rich veins	0.638
57	32O01	Troilus (Grid J4)	Worked deposit	18	537462	5652509	Dep. assoc. with porphyry intr.	0.825
58	32O01	Lac Troilus (Grid J3, Zone 87)	Active mine	18	537417	5651197	Dep. assoc. with porphyry intr.	0.799
59	32J15	Sondage n° 51-11-3	Worked deposit	18	532579	5635604	Copper-rich veins	0.729
60	32J15	Occurrence D	Showing	18	527079	5634479	Copper-rich veins	0.616
61	32J15	Troïlus Free Gold (Muscocho)	Dep. with tonnage est.	18	530238	5633005	Porphyry Cu-Au-Mo dep.	0.726
62	32J15	Zone M (Sondage W-4)	Worked deposit	18	529515	5632659	Copper-rich veins	0.787
63	32J15	Bergeron	Worked deposit	18	524454	5629703	Copper-rich veins	0.643
64	32J15	Laplante (Caro)	Worked deposit	18	522504	5629028	Copper-rich veins	0.580
65	32J15	Lac Frotet (Baie Ouest)	Worked deposit	18	534029	5625978	Copper-rich veins	0.610
66	32K12	Eider Zone Interne Est	Showing	18	318736	5614453	Dep. assoc. with porphyry intr.	0.689
67	32K12	Zone Interne Nord	Showing	18	317927	5614390	Cu-rich skarns assoc. with porphyry Cu	0.695
68	32K12	Eider Zone Contact Ouest	Showing	18	317927	5614095	Cu-rich skarns assoc. with porphyry Cu	0.708
69	32K12	Skarn à Magnétite	Showing	18	318143	5614028	Cu-rich skarns assoc. with porphyry Cu	0.716
70	32K11	H-1456-009	Worked deposit	18	333763	5610345	Dep. assoc. with porphyry intr.	0.599
71	32I04	Points d'intérêt No 8 (Lac Rita)	Showing	18	578805	5555829	Copper-rich veins	0.653
72	32J01	Atlas	Worked deposit	18	560280	5540853	Copper-rich veins	0.566

The 11 deposits highlighted in yellow were used to validate the results and were not used in processing. All the deposits are shown on the geological map in Figure 4. The Vfavor(m) value indicates the value measured for each deposit on the final favourability map.

APPENDIX 2

Favourability assessment for each parameter used in processing.

Table of parameters to assess mineral potential for porphyry Cu-Au ± Mo deposits in the Baie-James region

Distance (m) / Density (km²)	Surface (km²)	No. Points	W+	s(W+)	W-	s(W-)	Contrast	s(Contr.)	Cont. norm.	Vfavor	Ranking
Proximity to a heat source											
Proximity to a synvolcanic intrusion											
0 - 800	3283.04	8	1.9927	0.354	-0.1225	0.1374	2.1152	0.3797	5.5707	0.627	31
801 - 1600	703.8	3	2.5537	0.5786	-0.0466	0.1313	2.6003	0.5933	4.3828	0.656	
1601 - 2400	438.2	1	1.927	1.0011	-0.0141	0.1291	1.9411	1.0094	1.923	0.617	
2401 - 4001	178815.24	49	-0.1947	0.1429	2.0999	0.2891	-2.2946	0.3224	-7.1162	0.310	
Lithological control											
Proximity to a felsic or intermediate porphyry intrusion											
0 - 200	583.84	9	3.8505	0.3359	-0.1565	0.1387	4.007	0.3634	11.0252	0.741	26
201 - 400	728.32	5	3.0329	0.4488	-0.0816	0.1337	3.1145	0.4682	6.6516	0.687	
401 - 600	1165.72	4	2.336	0.5009	-0.0615	0.1325	2.3974	0.5181	4.6275	0.644	
601 - 10001	180762.4	43	-0.3362	0.1525	3.0899	0.2366	-3.426	0.2815	-12.172	0.217	
Proximity to a felsic or intermediate intrusion containing hematite and/or magnetite											
0 - 200	485.92	16	4.6274	0.2542	-0.3016	0.1491	4.929	0.2947	16.7248	0.796	22
201 - 400	661.6	6	3.3136	0.4101	-0.1	0.1349	3.4135	0.4317	7.9068	0.705	
401 - 1200	5541.24	16	2.1629	0.2504	-0.2736	0.1491	2.4364	0.2914	8.3614	0.646	
1201 - 10001	176551.52	23	-0.9384	0.2085	2.8424	0.1627	-3.7808	0.2645	-14.2953	0.187	
Structural control											
Proximity to a regional ductile fault											
0 - 2000	19698.16	31	1.5546	0.1797	-0.5961	0.1826	2.1507	0.2562	8.3941	0.629	30
2001 - 3000	7234.8	13	1.6874	0.2776	-0.1994	0.1444	1.8869	0.3129	6.0305	0.613	
3001 - 10001	156307.32	17	-1.1189	0.2425	1.5921	0.1509	-2.711	0.2856	-9.4906	0.276	
Density of regional ductile faults											
0.292 - 1.462	6904.92	16	1.9423	0.2503	-0.2659	0.1491	2.2081	0.2913	7.5795	0.633	29
0 - 0.292	176335.36	45	-0.2659	0.1491	1.9423	0.2503	-2.2081	0.2913	-7.5795	0.317	
Density of faulting											
18.84 - 37.24	3.88	1	6.9496	1.1607	-0.0165	0.1291	6.9661	1.1679	5.9648	0.918	7
7.01 - 18.84	22.76	1	4.9273	1.0227	-0.0164	0.1291	4.9437	1.0308	4.7958	0.797	
1.17 - 7.01	264.68	11	4.8692	0.308	-0.1975	0.1414	5.0666	0.3389	14.95	0.804	
0.318 - 1.17	2434.56	16	2.989	0.2508	-0.2909	0.1491	3.2799	0.2918	11.2407	0.697	
0 - 0.318	180514.4	32	-0.6303	0.1768	3.4748	0.1867	-4.1051	0.2571	-15.9659	0.160	
Density of fracturing											
2.54 - 5.73	16.96	1	5.2373	1.0309	-0.0164	0.1291	5.2537	1.0389	5.057	0.815	18
0.94 - 2.54	98.08	2	4.1353	0.7144	-0.0328	0.1302	4.1681	0.7262	5.7397	0.750	
0.32 - 0.94	639.36	6	3.3481	0.4102	-0.1001	0.1349	3.4481	0.4318	7.9859	0.707	
0 - 0.32	182485.88	52	-0.1556	0.1387	3.5907	0.3353	-3.7462	0.3629	-10.3233	0.190	
Density of quartz veining											
4.14 - 8.28	24.72	2	5.5772	0.7376	-0.0332	0.1302	5.6105	0.749	7.4908	0.837	13
1.58 - 4.14	349.16	7	4.118	0.3818	-0.12	0.1361	4.238	0.4053	10.4553	0.754	
0.01 - 1.58	5045	16	2.257	0.2504	-0.2764	0.1491	2.5333	0.2914	8.693	0.652	
0 - 0.01	177821.4	36	-0.4975	0.1667	2.6332	0.2005	-3.1307	0.2607	-12.0083	0.241	
Proximity to a brecciated texture											
0 - 1200	1085.28	25	4.2599	0.2023	-0.5215	0.1667	4.7815	0.2622	18.239	0.787	23
1201 - 2400	2271.56	6	2.0735	0.4088	-0.0911	0.1349	2.1646	0.4305	5.0286	0.630	
2401 - 10001	179883.44	30	-0.6914	0.1826	3.3319	0.1804	-4.0232	0.2567	-15.6725	0.167	
Evidence of hydrothermal activity in the bedrock											
Indicator metal analyses											
Proximity to a copper anomaly ≥ 1000 ppm											
0 - 200	93	34	7.4562	0.2153	-0.8147	0.1925	8.2709	0.2888	28.6391	0.997	2
201 - 600	296.32	7	4.2857	0.3825	-0.1203	0.1361	4.406	0.406	10.8522	0.765	
601 - 1000	506.84	6	3.5828	0.4107	-0.1008	0.1349	3.6836	0.4323	8.5217	0.721	
1001 - 1600	912.68	2	1.8863	0.7079	-0.0284	0.1302	1.9147	0.7198	2.6601	0.615	
1601 - 10001	181431.44	12	-1.6163	0.2887	4.4262	0.1448	-6.0425	0.323	-18.7087	0.001	
Proximity to a gold anomaly ≥ 100 ppb											
0 - 200	137.6	25	6.5024	0.2211	-0.5267	0.1667	7.0291	0.2769	25.3866	0.922	6
201 - 400	156.08	4	4.3692	0.5065	-0.067	0.1325	4.4362	0.5236	8.473	0.766	
401 - 1600	2010.08	10	2.709	0.317	-0.1681	0.14	2.8771	0.3466	8.3014	0.673	
1601 - 2400	1784.72	6	2.3155	0.4089	-0.0938	0.1349	2.4092	0.4306	5.5951	0.645	
2401 - 10001	179151.8	16	-1.316	0.25	3.5091	0.1499	-4.8251	0.2915	-16.5524	0.101	
Proximity to a molybdenum anomaly ≥ 21 ppm											
0 - 200	27.2	14	8.0662	0.3836	-0.2607	0.1459	8.3268	0.4104	20.2872	1.000	1
201 - 600	104.12	7	5.3773	0.3913	-0.1214	0.1361	5.4987	0.4143	13.2709	0.830	
601 - 1600	546.48	5	3.3225	0.4493	-0.0826	0.1337	3.405	0.4687	7.2644	0.704	
1601 - 10001	182562.48	35	-0.552	0.169	4.7857	0.2	-5.3377	0.2619	-20.3834	0.058	
Proximity to a silver anomaly ≥ 3 ppm											
0 - 200	66.88	25	7.4914	0.2527	-0.5271	0.1667	8.0185	0.3028	26.4852	0.981	3
201 - 800	422.28	11	4.386	0.3055	-0.1966	0.1414	4.5826	0.3367	13.6115	0.775	
801 - 1600	1062.6	7	2.9914	0.3792	-0.1161	0.1361	3.1075	0.4029	7.7128	0.687	
1601 - 2600	1846.2	6	2.2815	0.4089	-0.0934	0.1349	2.3749	0.4306	5.5157	0.643	
2601 - 10001	179842.32	12	-1.6075	0.2887	3.7828	0.1439	-5.3903	0.3226	-16.7109	0.054	
Proximity to an arsenic anomaly ≥ 48 ppm											
0 - 200	81.32	7	5.6449	0.3954	-0.1215	0.1361	5.7664	0.4181	13.7907	0.846	11
201 - 400	97.64	4	4.8542	0.5106	-0.0673	0.1325	4.9215	0.5275	9.3303	0.796	
401 - 800	349.88	4	3.5475	0.5029	-0.0659	0.1325	3.6135	0.52	6.9485	0.717	
801 - 2600	3053.28	10	2.2892	0.3167	-0.1623	0.14	2.4515	0.3463	7.0787	0.647	
2601 - 10001	179658.16	36	-0.5077	0.1667	3.0495	0.2007	-3.5573	0.2609	-13.635	0.206	
Proximity to a tungsten anomaly ≥ 5 ppm											
0 - 200	55.44	8	6.2273	0.3822	-0.1403	0.1374	6.3676	0.4061	15.6783	0.882	9
201 - 600	209.32	4	4.0691	0.5048	-0.0667	0.1325	4.1358	0.5219	7.9239	0.748	
601 - 2400	2430.48	12	2.7014	0.2894	-0.2058	0.1429	2.9071	0.3227	9.0077	0.675	
2401 - 10001	180545.04	37	-0.4853	0.1644	3.2951	0.205	-3.7804	0.2628	-14.3839	0.187	

Value or Distance = Class ID or value of specified attribute; **Surface (km²)** = Surface area of each class in km²; **No_Points** = Number of measurement points lying within the surface area of the class; **W+** = W+ value; **s(W+)** = Standard deviation of W+; **W- =** W- value; **s(W-)** = Standard deviation of W-; **Contrast** = Contrast (difference between W+ and W-); **s(Contrast)** = Standard deviation of C; **Cont_norm** = Normalized contrast (C value divided by s(C)); **Vfavor**[1] = Calculated favourability value; **Ranking** = Order of the parameter favourabiity.

1 The Vfavor parameter is not calculated with ArcSDM. See section entitled ''Methodology''.

APPENDIX 2

Favourability assessment for each parameter used in processing (continued).

Table of parameters to assess mineral potential for porphyry Cu-Au ± Mo deposits in the Baie-James region (continued)

Distance (m)	Surface (km²)	No. Points	W+	s(W+)	W-	s(W-)	Contraste	s(Contr.)	Cont. norm.	Vfavor	Rang
Proximity to an alteration indicator mineral											
Proximity to a potassic alteration indicator mineral											
0 - 200	129.48	9	5.4131	0.3456	-0.159	0.1387	5.5721	0.3724	14.9644	0.835	14
200 - 1200	1257.84	10	3.1808	0.3175	-0.1722	0.14	3.353	0.347	9.6625	0.701	
1201 - 2400	2364.44	14	2.884	0.2681	-0.2478	0.1459	3.1319	0.3052	10.2623	0.688	
2401 - 3400	2466.12	7	2.1457	0.3785	-0.1084	0.1361	2.2541	0.4022	5.604	0.635	
3401 - 10001	177022.4	21	-1.032	0.2182	2.9675	0.1586	-3.9995	0.2698	-14.8246	0.169	
Proximity to a chloritic alteration indicator mineral											
0 - 200	286.4	12	4.8777	0.2949	-0.2176	0.1429	5.0952	0.3277	15.5481	0.806	21
201 - 400	325.52	4	3.6206	0.5031	-0.0661	0.1325	3.6866	0.5202	7.0863	0.721	
401 - 1000	1721.4	7	2.5064	0.3787	-0.1125	0.1361	2.6189	0.4024	6.5075	0.657	
1001 - 10001	180906.96	38	-0.4606	0.1622	3.3977	0.2095	-3.8583	0.265	-14.5588	0.181	
Proximity to an epidotization indicator mineral											
0 - 200	99.4	5	5.0692	0.4589	-0.085	0.1337	5.1543	0.478	10.7836	0.810	20
201 - 400	133.56	3	4.2341	0.5839	-0.0497	0.1313	4.2838	0.5985	7.1573	0.757	
401 - 1800	2502.44	11	2.5846	0.3022	-0.1852	0.1414	2.7698	0.3336	8.3017	0.666	
1801 - 2800	2576.76	7	2.1017	0.3785	-0.1078	0.1361	2.2095	0.4022	5.4933	0.633	
2801 - 10001	177928.12	35	-0.5262	0.169	2.6926	0.1966	-3.2188	0.2593	-12.4144	0.234	
Proximity to a silicification indicator mineral											
0 - 200	86.84	13	6.2704	0.3008	-0.2393	0.1444	6.5097	0.3336	19.512	0.891	8
201 - 1600	1612.76	13	3.1947	0.2785	-0.2309	0.1444	3.4256	0.3137	10.9211	0.706	
1601 - 2600	1873.12	7	2.4216	0.3787	-0.1117	0.1361	2.5333	0.4024	6.2956	0.652	
2601 - 10001	179667.56	28	-0.7592	0.189	3.3321	0.1749	-4.0912	0.2575	-15.8883	0.161	
Proximity to hematite or magnetite alteration											
0 - 200	149.84	13	5.6535	0.2902	-0.2389	0.1444	5.8924	0.3241	18.1783	0.854	10
201 - 400	197.32	6	4.5452	0.4146	-0.1025	0.1349	4.6477	0.436	10.6602	0.779	
401 - 1200	1638.92	11	3.0102	0.3025	-0.1899	0.1414	3.2001	0.334	9.5823	0.692	
1201 - 10001	181254.2	31	-0.6662	0.1796	3.8298	0.184	-4.496	0.2571	-17.4863	0.128	
Proximity to an anomalous NORMAT alteration index											
Proximity to an anomalous ISER index											
0 - 400	131.16	10	5.5128	0.329	-0.1784	0.14	5.6912	0.3576	15.9157	0.842	12
401 - 1000	413.68	11	4.4071	0.3056	-0.1967	0.1414	4.6037	0.3367	13.6713	0.776	
1001 - 1800	761.4	6	3.1719	0.4099	-0.0994	0.1349	3.2713	0.4315	7.5814	0.696	
1801 - 10001	181934.04	34	-0.5775	0.1715	4.1492	0.1945	-4.7267	0.2593	-18.2286	0.109	
Proximity to an anomalous ICHLO index											
0 - 200	55.84	3	5.1387	0.5935	-0.0501	0.1313	5.1888	0.6079	8.5361	0.812	19
201 - 1200	744.72	13	3.9769	0.2798	-0.2357	0.1444	4.2126	0.3148	13.3797	0.753	
1201 - 2400	1563.32	6	2.4484	0.409	-0.095	0.1349	2.5434	0.4307	5.9053	0.653	
2401 - 10001	180876.4	39	-0.4344	0.1601	3.3397	0.2142	-3.7741	0.2674	-14.1117	0.188	
Proximity to sulphide or oxide mineralization											
Proximity to arsenopyrite mineralizaton											
0 - 200	29.4	2	5.39	0.7325	-0.0332	0.1302	5.4231	0.7439	7.2897	0.826	17
201 - 1200	413.52	2	2.6806	0.7088	-0.0311	0.1302	2.7117	0.7207	3.7627	0.663	
1201 - 7800	9903.52	22	1.9	0.2134	-0.3919	0.1601	2.2918	0.2668	8.5888	0.638	
7801 - 10001	172893.84	35	-0.4975	0.169	2.0236	0.1964	-2.5211	0.2591	-9.73	0.291	
Proximity to bornite mineralization											
0 - 600	17.4	8	7.8461	0.481	-0.1405	0.1374	7.9866	0.5003	15.965	0.980	4
601 - 1200	50.4	3	5.2473	0.5953	-0.0502	0.1313	5.2975	0.6097	8.6894	0.818	
1201 - 2000	120.4	1	3.2249	1.0042	-0.0159	0.1291	3.2407	1.0124	3.2009	0.695	
2001 - 10001	183052.08	49	-0.2181	0.1429	5.3206	0.2983	-5.5387	0.3308	-16.7439	0.042	
Proximity to chalcopyrite mineralization											
0 - 200	108.88	24	6.7442	0.2312	-0.4995	0.1644	7.2437	0.2837	25.5336	0.935	5
201 - 400	132.68	4	4.5363	0.5077	-0.0671	0.1325	4.6034	0.5247	8.7733	0.776	
401 - 1000	847.72	2	1.9603	0.7079	-0.0287	0.1302	1.989	0.7198	2.7632	0.619	
1001 - 10001	182151	31	-0.6711	0.1796	4.4432	0.1851	-5.1143	0.258	-19.8263	0.077	
Proximity to magnetite mineralization											
0 - 200	694.28	15	4.1944	0.261	-0.2785	0.1475	4.4729	0.2998	14.9193	0.769	25
201 - 400	881.56	6	3.0242	0.4096	-0.0987	0.1349	3.123	0.4313	7.2413	0.688	
401 - 600	1488.88	5	2.3144	0.448	-0.0774	0.1337	2.3918	0.4675	5.1163	0.644	
601 - 10001	180175.56	35	-0.5388	0.169	3.2463	0.197	-3.785	0.2596	-14.583	0.187	
Proximity to molybdenite mineralization											
0 - 1000	114.96	4	4.6845	0.5089	-0.0672	0.1325	4.7517	0.5259	9.0355	0.785	24
1001 - 2000	306.56	2	2.9816	0.7094	-0.0317	0.1302	3.0133	0.7213	4.1777	0.681	
2001 - 3000	498.96	2	2.492	0.7085	-0.0306	0.1302	2.5226	0.7204	3.5017	0.651	
3001 - 20001	182319.8	53	-0.1356	0.1374	3.2706	0.3551	-3.4062	0.3807	-8.9461	0.218	
Proximity to pyrite mineralization											
0 - 200	477.52	24	5.0684	0.2095	-0.4975	0.1644	5.5658	0.2663	20.9023	0.834	15
201 - 400	604.2	3	2.707	0.5788	-0.0471	0.1313	2.7542	0.5935	4.6406	0.665	
401 - 600	1009.8	2	1.785	0.7078	-0.0278	0.1302	1.8128	0.7197	2.5189	0.609	
601 - 10001	181148.76	32	-0.6338	0.1768	3.743	0.187	-4.3768	0.2573	-17.0078	0.138	
Proximity to pyrrhotite mineralization											
0 - 200	218.72	13	5.2458	0.286	-0.2385	0.1444	5.4843	0.3203	17.1199	0.829	16
201 - 400	264.12	5	4.0595	0.4515	-0.0841	0.1337	4.1436	0.4709	8.7998	0.749	
401 - 1600	3362.4	16	2.6643	0.2506	-0.2858	0.1491	2.9501	0.2916	10.1171	0.677	
1601 - 10001	179395.04	27	-0.794	0.1925	3.288	0.1723	-4.082	0.2583	-15.8036	0.162	
Evidence of mineralization in the secondary environment											
Proximity to a copper anomaly											
0 - 1000	1097.8	11	3.4142	0.303	-0.1929	0.1414	3.6071	0.3344	10.7864	0.717	27
1001 - 2600	4931.52	13	2.0715	0.2777	-0.2125	0.1444	2.284	0.313	7.2972	0.637	
2601 - 10001	177210.96	37	-0.4666	0.1644	2.485	0.2045	-2.9516	0.2624	-11.2476	0.256	
Proximity to a gold anomaly											
0 - 1000	1227.84	3	1.9954	0.5781	-0.0437	0.1313	2.0391	0.5928	3.4399	0.622	32
1001 - 1800	2362.84	5	1.8513	0.4477	-0.0726	0.1337	1.9239	0.4672	4.1177	0.616	
1801 - 3200	6467.32	9	1.4314	0.3336	-0.1237	0.1387	1.5552	0.3613	4.305	0.593	
3201 - 10001	173182.28	44	-0.2703	0.1508	1.6261	0.2427	-1.8964	0.2858	-6.6366	0.343	
Proximity to a molybdenum anomaly											
0 - 800	2800.68	13	2.6393	0.278	-0.2243	0.1444	2.8637	0.3132	9.142	0.672	28
801 - 1400	4979.44	11	1.8944	0.3018	-0.1714	0.1414	2.0657	0.3333	6.1971	0.624	
1401 - 10001	175460.16	37	-0.4567	0.1644	2.2292	0.2044	-2.6859	0.2624	-10.2376	0.278	

APPENDIX 3

Inference model of the potential for porphyry Cu-Au ± Mo deposits in the Baie-James region.

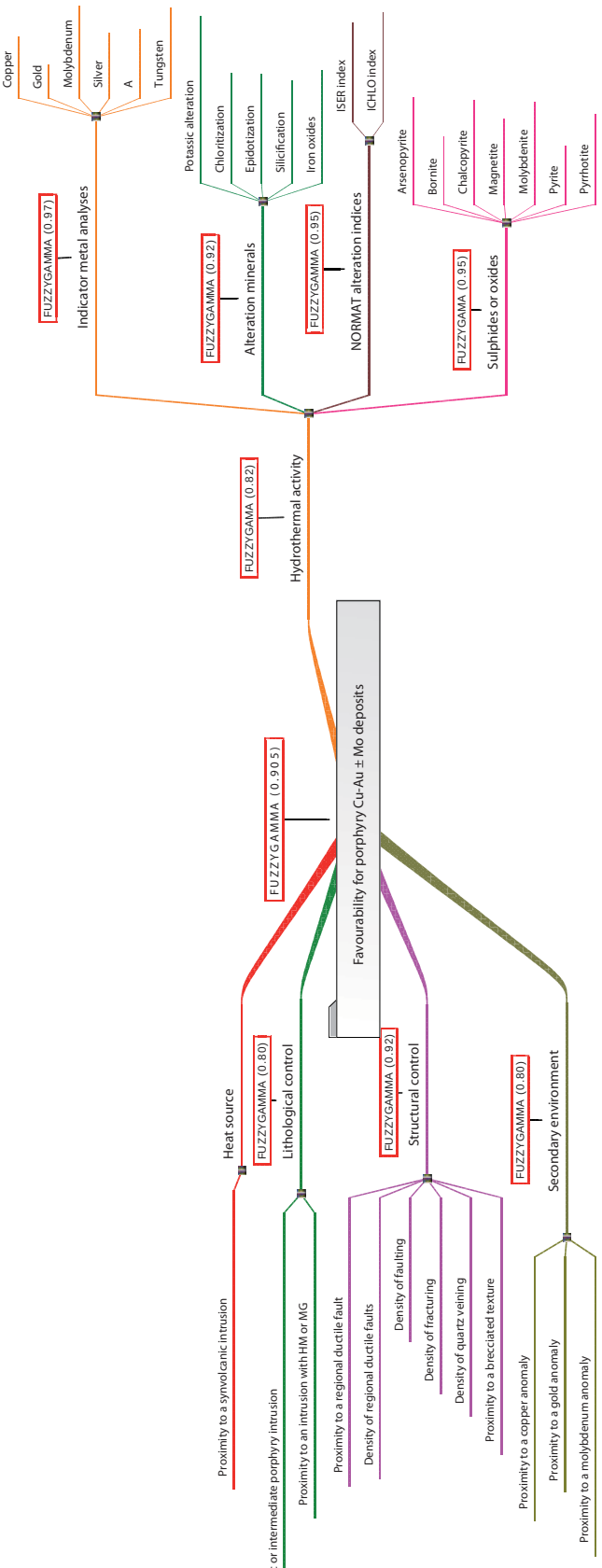

This inference model illustrates the parameter combination process. The various parameters and the sub-sets were all combined using FUZZYGAMMA operators. Numbers in parentheses indicated after each FUZZYGAMMA operator represent the factor used to calibrate the parameter or sub-set so as to obtain a background value on the final map of about 0.5. HM = hematite; MG = magnetite. The resulting favourability maps may be downloaded in PDF format by clicking on the appropriate map area in the location maps shown in Appendix 4.

Favourability maps for porphyry Cu-Au ± Mo deposits in the Baie-James region.

Favourability map at a scale of 1/500,000

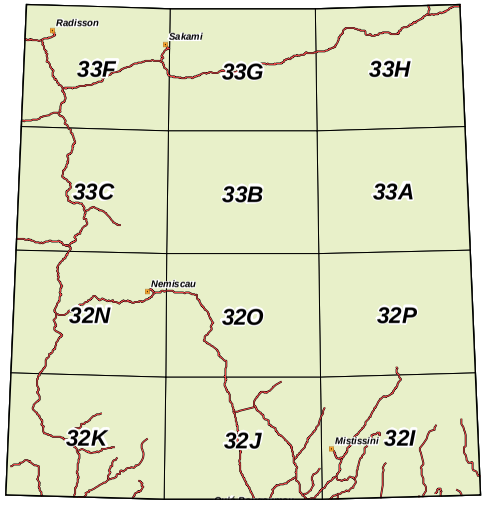

Favourability map at a scale of 1/250,000

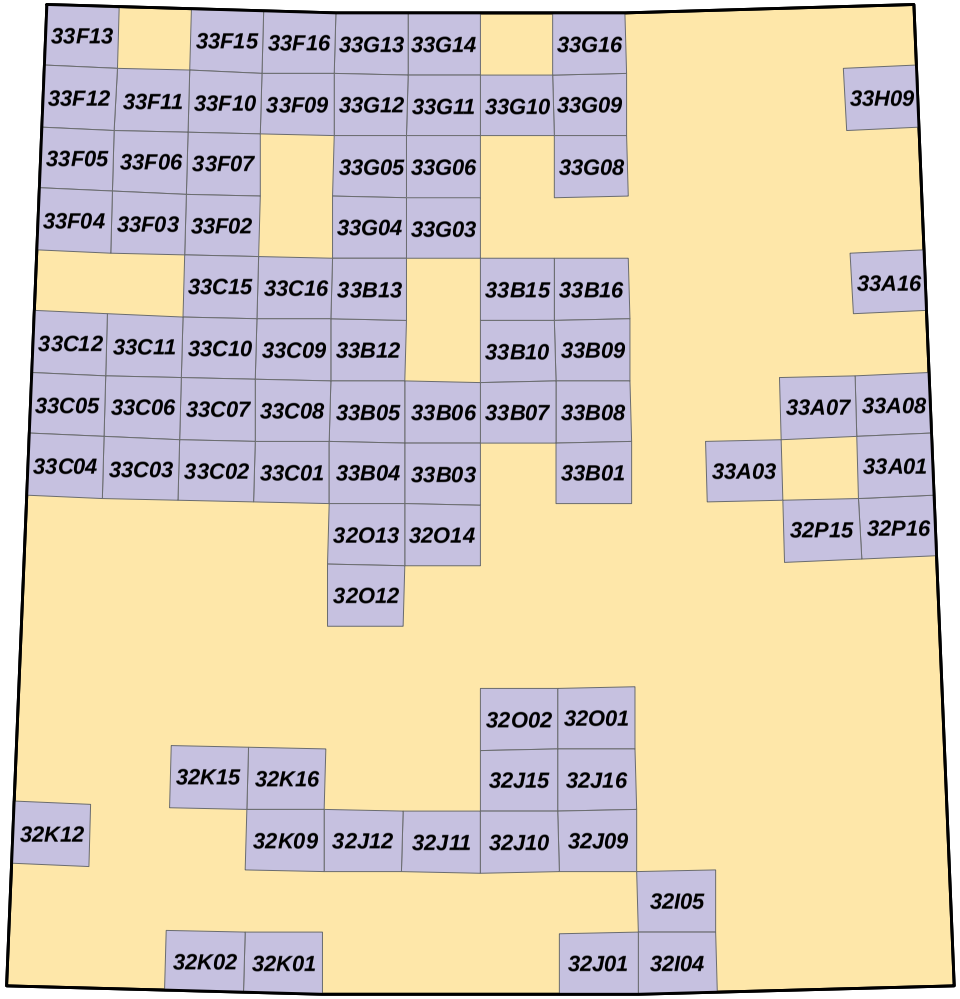

Favourability maps at a scale of 1/50,000

Ressources naturelles et Faune
Québec